SMALL SCALE CREATION IN ACTIVE SCALARS

ALEXANDER KISELEV

Abstract. The focus of the course is on small scale formation in solutions of the incompressible Euler equation of fluid dynamics and associated models. We first review the regularity results and examples of small scale growth in two dimensions. Then we discuss a specific singular scenario for the three dimensional Euler equation discovered by Hou and Luo, and analyze some associated models. Finally, we will also consider the surface quasi-geostrophic (SQG) equation, and review the construction an example of singularity formation in the modified SQG patch solutions as well as discuss example of unbounded growth of derivatives for the smooth solutions.

1. Introduction

In this section we briefly set the stage; for more detailed introduction into our subject here one may consult excellent textbooks [44] or [46]. The incompressible Euler equation of fluid mechanics goes back to 1755 [25]. It appears to be the second PDE ever written down. The equation describes motion of inviscid and incompressible (also called ideal) fluid. The Euler equation is a close relative of the Navier-Stokes equations of fluid mechanics, which came about almost one hundred years later and include viscous effects. One could argue that the Euler equation is less relevant in applications - for example, an observation due to D'Alambert is that there is neither drag nor lift on a body moving in an irrotational ideal fluid. However, Euler equation contains the fluid mechanics nonlinearity, the heart of the Navier-Stokes, and thus for a mathematician it is the first equation to understand. It is also a model of choice in a variety of situations where viscous effects can be ignored. The equation is given by

$$\partial_t u + (u \cdot \nabla) u = \nabla p, \;\; \nabla \cdot u = 0. \tag{1.1}$$

Here $u(x,t)$ is the vector field of the flow, and $p(x,t)$ is pressure. When set in a domain D with boundary, the boundary condition that is natural in many instances is no penetration, $u \cdot n|_{\partial D} = 0$.

The story on global regularity vs finite time singularity formation question for the Euler equation is very different in two and three dimensions. To see why, it is convenient to look at vorticity $\omega = \mathrm{curl} u$. In the vorticity form, the Euler equation becomes

$$\partial_t \omega + (u \cdot \nabla)\omega = (\omega \cdot \nabla) u, \tag{1.2}$$

which is supplemented with the Biot-Savart law which allows to express the velocity u through vorticity. In two dimensions, the Biot-Savart law takes form $u = \nabla^\perp (-\Delta_D)^{-1}\omega$, where Δ_D is

2010 *Mathematics Subject Classification.* 35Q35,76B03.

Key words and phrases. Euler equation, SQG equation, two-dimensional incompressible flow, small scale creation, derivatives growth, weak turbulence, double exponential growth, hyperbolic flow.

Department of Mathematics, Duke University, 120 Science Dr., Durham NC 27708, USA; email: kiselev@math.duke.edu.

the Dirichlet Laplacian on domain D or simply Laplacian on $\mathbb{R}^2$ or $\mathbb{T}^2$, and $\nabla^\perp = (\partial_{x_2}, -\partial_{x_1})$. In three dimensions, $u = \mathrm{curl}(-\Delta)^{-1}\omega$ in $\mathbb{R}^3$ or $\mathbb{T}^3$, while in bounded domains the Biot-Savart law in general takes more complicated form (see [24]).

Coming back to (1.2), notice that the term on the right hand side vanishes in two dimensions. This makes equation simpler; notice that for any smooth solution and $p \geq 1$ we have

$$\partial_t \int_D |\omega(x,t)|^p\,dx = p\int_D |\omega|^{p-1}\,\mathrm{sgn}(\omega)\partial_t\omega\,dx = -\int_D u\cdot\nabla|\omega|^p\,dx = \int_D (\nabla\cdot u)|\omega|^p\,dx = 0;$$

where the third step is obtained integrating by parts (using the boundary condition) and the last one by substituting $\nabla \cdot u = 0$. This observation yields many conserved quantities that in three dimensional case are lacking.

In the next section, we overview existence and uniqueness theory for a fairly general class of solutions to the 2D Euler equation, called Yudovich theory.

2. The 2D Euler equation: a sketch of Yudovich theory

In this section, we assume that $D \subset \mathbb{R}^2$ is a smooth bounded domain or that solutions are periodic in space (i.e. $D = \mathbb{T}^2$). More details on the material of this section can be found in [39, 44, 46]. A classical solution of the 2D Euler equation is a C^1 function ω that solves

$$\partial_t\omega + (u\cdot\nabla)\omega = 0, \;\; u = \nabla^\perp(-\Delta_D)^{-1}\omega, \;\; \omega(x,0) = \omega_0(x). \tag{2.1}$$

It turns out that one can define unique solutions for more general classes of the initial data if one properly modifies the notion of solution.

A key object of the Yudovich theory are particle trajectories $\Phi_t(x)$:

$$\frac{d\Phi_t(x)}{dt} = u(\Phi_t(x),t), \;\; \Phi_0(x) = x \tag{2.2}$$

which are defined by incompressible vector field u. If u is smooth, then so is the map $\Phi_t(x)$; this map is also measure preserving since u is divergence free. The map is one-to-one on D by uniqueness of solutions to ordinary differential equations with Lipschitz coefficients. It is not hard to see that it is also onto by solving (2.2) backward in time.

A direct calculation shows that ω remains constant on trajectories (again, for smooth solutions), namely, $\frac{d}{dt}\omega(\Phi_t(x),t) = 0$, so

$$\omega(x,t) = \omega_0(\Phi_t^{-1}(x)). \tag{2.3}$$

Next, denote by $G_D(x,y)$ the Green's function of the Dirichlet Laplacian in domain D, so that

$$u(x,t) = \int_D \nabla^\perp G_D(x,y)\omega(y)\,dy. \tag{2.4}$$

A C^1 solution of the Euler equation satisfies the system (2.2), (2.3), and (2.4). We are going to define solutions of low regularity, with ω just in L^∞, by using (2.2), (2.3) and (2.4) instead of (2.1). At the heart of the argument are a few simple observations. The first one is a well known estimate of potential theory.

Proposition 2.1. *If $D \subset \mathbb{R}^2$ is a compact domain with a smooth boundary, the Dirichlet Green's function $G_D(x,y)$ has the form*

$$G_D(x,y) = \frac{1}{2\pi}\log|x-y| + h(x,y).$$

Here, for each $y \in D$, $h(x,y)$ is a harmonic function solving

$$\Delta_x h = 0, \quad h|_{x\in\partial D} = -\frac{1}{2\pi}\log|x-y|. \tag{2.5}$$

We have $G_D(x,y) = G_D(y,x)$ for all $(x,y) \in D$, and $G_D(x,y) = 0$ if either x or y belongs to ∂D. In addition, we have the estimates

$$|G_D(x,y)| \le C(D)\left(|\log|x-y|| + 1\right) \tag{2.6}$$

$$|\nabla G_D(x,y)| \le C(D)|x-y|^{-1}, \tag{2.7}$$

$$|\nabla^2 G_D(x,y)| \le C(D)|x-y|^{-2}. \tag{2.8}$$

The following lemma is a consequence of Proposition 2.1.

Lemma 2.2. *The kernel $K_D(x,y) = \nabla^\perp G_D(x,y)$ satisfies*

$$\int_D |K_D(x,y) - K_D(x',y)|\, dy \le C(D)\phi(|x-x'|), \tag{2.9}$$

where

$$\phi(r) = \begin{cases} r(1-\log r) & r < 1 \\ 1 & r \ge 1, \end{cases} \tag{2.10}$$

with a constant $C(D)$ which depends only on the domain D.

Proof. Set $|x-x'| = r > 0$, split the integration into $B_{2r}(x) \cap D$ and its complement, and use estimates of the Proposition 2.1. We leave details to the interested reader, they can also be found in [39, 46]. □

A result on the regularity of fluid velocity is an immediate consequence.

Corollary 2.3. *Lt D be smooth bounded domain. Suppose the vorticity ω is bounded. Then fluid velocity u satisfies*

$$\|u\|_{L^\infty} \le C(D)\|\omega\|_{L^\infty}, \tag{2.11}$$

and

$$|u(x) - u(x')| \le C\|\omega\|_{L^\infty}\phi(|x-x'|), \tag{2.12}$$

with the function $\phi(r)$ defined in (2.10).

Proof. The estimate (2.11) follows from (2.7). The proof of (2.12) is immediate from Lemma 2.2, as

$$u(x,t) = \int_D K_D(x,y)\omega(y,t)dy.$$

□

We say that u is log-Lipschitz if it satisfies (2.12). A key component of the Yudovich theory is the analysis of the fluid particle trajectories (2.2). The classical requirement for uniqueness of solutions to a system of ODE is Lipschitz dependence of coefficients on the unknowns. If the vorticity is bounded, heuristically we expect the velocity u to be one derivative more regular, which would just match the requirement. However, the L^∞ is the endpoint setting, where we lose a logarithm in regularity, leading to estimates on velocity that are just log-Lipschitz. We will see later that this estimate is sharp and one cannot in general expect better regularity of the velocity corresponding to bounded vorticity. A key observation of the Yudovich theory is that we can still define fluid particle trajectories (2.2) uniquely if the velocity u is only log-Lischitz.

The following lemma addresses this question [39, 46].

Lemma 2.4. *Let D be a bounded smooth domain in $\mathbb{R}^d$. Assume that the velocity field $b(x,t)$ satisfies, for all $t \geq 0$:*

$$b \in C([0,\infty) \times \bar{D}), \;\; |b(x,t) - b(y,t)| \leq C\phi(|x-y|), \;\; b(t,x) \cdot \nu|_{\partial D} = 0. \tag{2.13}$$

Here, the function $\phi(r)$ is given by (2.10) and ν is the unit normal to ∂D at point x. Then the Cauchy problem in $\bar{D}$

$$\frac{dx}{dt} = b(x,t), \;\; x(0) = x_0, \tag{2.14}$$

has a unique global solution. Moreover, if $x_0 \notin \partial D$, then $x(t) \notin \partial D$ for all $t \geq 0$. If $x_0 \in \partial D$, then $x(t) \in \partial D$ for all $t \geq 0$.

Note that the log-Lipschitz regularity is essentially border-line: the familiar example of the ODE

$$\dot{x} = x^\beta, \;\; x(0) = 0,$$

with $\beta \in (0,1)$ does not have the uniqueness property: for example, $x(t) \equiv 0$, and

$$x(t) = \frac{t^p}{p^p}, \;\; p = \frac{1}{1-\beta}$$

are both solutions (and in fact one can find infinitely many solutions by separating from zero at an arbitrary time). Thus ODEs with just Hölder (with an exponent smaller than one) coefficients may have more than one solution. Existence of the solutions, on the other hand, does not really require the log-Lipschitz condition: uniform continuity of $b(x,t)$ and at most linear growth as $|x| \to +\infty$ would be sufficient, see e.g. [11] for the Peano existence theorem. We omit the proof of Lemma 2.4, one can check [46] for details.

Now an iterative scheme can be used to construct a weak solution to the 2D Euler equation with L^∞ vorticity, using (2.2), (2.3), and (2.4). We summarize the results of Yudovich theory in the following theorems.

Theorem 2.5. *Fix any $\omega_0 \in L^\infty(D)$. There exists the unique triple $(\omega(x,t), u(x,t), \Phi_t(x))$ satisfying (2.2), (2.3) and (2.4) such that for every $T > 0$ the vorticity ω belongs to $L^\infty([0,T], L^\infty(D))$ and is weak-$*$ continuous in time in L^∞, the fluid velocity $u(t,x)$ is uniformly bounded and log-Lipschitz in x and t, and $\Phi_t \in C^{\alpha(T)}([0,T] \times \bar{D})$ is measure preserving, invertible mapping of $\bar{D}$, satisfying*

$$\frac{d\Phi_t(x)}{dt} = u(\Phi_t(x), t), \;\; \Phi_0(x) = x, \tag{2.15}$$

$$\omega(x,t) = \omega_0(\Phi_t^{-1}(x)),$$
$$u(x,t) = \int_D K_D(x,y)\omega(y,t)\,dy.$$

Here $\alpha(T) > 0$ and only depends on $\|\omega_0\|_{L^\infty}$ and time T.

A triple (ω, u, Φ_t) satisfying the conditions of Theorem 2.5 is called Yudovich solution to the 2D Euler equation.

If the initial data ω_0 is more regular, this regularity is inherited by the solution.

Theorem 2.6. *Suppose that $\omega_0 \in C^k(\bar{D})$, $k \geq 1$. Then the solution described in Theorem 2.5, satisfies, in addition, the following regularity properties, for each $t \geq 0$:*

$$\omega(t) \in C^k(\bar{D}),\ \ \Phi_t(x) \in C^{k,\alpha(t)}(\bar{D}),\ \ \text{and } u \in C^{k,\beta}(\bar{D}),$$

for all $\beta < 1$. In addition, the kth order derivatives of u are log-Lipschitz.

An important example of a Yudovich solution of the 2D Euler equations is the "singular cross" flow, considered by Bahouri and Chemin [1]. We discuss its periodic version here. It corresponds to the vorticity ω_0 which equals to (-1) in the first and third quadrants of the torus $(-\pi,\pi] \times (-\pi,\pi]$, and to $(+1)$ in the other two quadrants:

$$\begin{aligned} &\omega_0(x_1,x_2) = -1 \text{ for } \{0 < x_1, x_2 < \pi\} \text{ and } \{-\pi \leq x_1, x_2 < 0\}, \\ &\omega_0(x_1,x_2) = 1 \text{ for } \{0 < x_1 < \pi,\ -\pi < x_2 < 0\}, \text{ and } \{-\pi < x_1 < 0,\ 0 < x_2 < \pi\}. \end{aligned} \tag{2.16}$$

We set ω_0 to be equal to zero on the separatrices $x_{1,2} = 0, \pi$. The singular cross has four vortices, one in each quadrant of the torus, and a hyperbolic point at the origin. In fact, ω_0 is a stationary Yudovich solution of the Euler equations. To arrive at this conclusion, the key observation is that ω_0 has the symmetries

$$\omega_0(x_1,x_2) = -\omega_0(-x_1,x_2) = -\omega_0(x_1,-x_2) \tag{2.17}$$

on the torus $(-\pi,\pi] \times (-\pi,\pi]$.

Lemma 2.7. *If the initial condition $\omega_0 \in L^\infty$, and satisfies the symmetries (2.17), then the Yudovich solution of the 2D Euler equations satisfies the same symmetries for all $t \geq 0$:*

$$\omega(x_1,x_2,t) = -\omega(-x_1,x_2,t) = -\omega(x_1,-x_2,t). \tag{2.18}$$

The lemma is proved by checking that if $\omega(x_1,x_2,t)$ is a Yudovich solution of the 2D Euler equation, then so is $-\omega(-x_1,x_2,t)$, and then appealing to the uniqueness property to establish that $\omega(x_1,x_2,t) = -\omega(-x_1,x_2,t)$.

Given odd symmetry and periodicity of $\omega(x,t)$, it is not hard to check that the stream function $\psi := (-\Delta)^{-1}\omega$ is also odd with respect to both variables, with respect to zero as well as $\pm\pi$. Then $u_1 = \partial_{x_2}\psi$ is odd with respect to $x_1 = 0, \pm\pi$ and $u_2 = -\partial_{x_1}\psi$ is odd with respect to $x_2 = 0, \pm\pi$. This implies that the trajectories never leave the quadrants where they originate, and thus by (2.3) and (2.16) the solution is stationary: $\omega(x,t) \equiv \omega_0(x)$.

The singular cross flow has remarkable properties showing that the estimates on the Yudovich solution of Theorem 2.5 are qualitatively sharp. Namely, the following proposition holds:

Proposition 2.8. *Consider the singular cross solution described above. Then, for small positive x_1, we have*

$$u_1(x_1,0) = \frac{2}{\pi} x_1 \log x_1 + O(x_1). \tag{2.19}$$

The estimate (2.19) corresponds to u_1 being just log-Lipschitz near the origin. The proof of (2.19) is based on the periodic version of the Biot-Savart law:

Proposition 2.9. *Let $\omega \in L^\infty(\mathbb{T}^2)$ be a mean zero function. Then the vector field*

$$u = \nabla^\perp (-\Delta)^{-1}\omega \tag{2.20}$$

is given by

$$u(x) = -\frac{1}{2\pi}\lim_{\gamma\to 0}\int_{\mathbb{R}^2} \frac{(x-y)^\perp}{|x-y|^2}\omega(y)e^{-\gamma|y|^2}\,dy, \tag{2.21}$$

where ω has been extended periodically to all $\mathbb{R}^2$.

We leave the proof of this formula as an exercise.

Proof of Proposition 2.8. Given (2.21), one can show (2.19) by first estimating that the integral over the complement of the central period cell $(-\pi,\pi]$ contributes regular Lipschitz term to u_1 near the origin. As far as the integral over the central cell goes, let us denote it $u_1^C(x_1,0)$. It is convenient to go back to representation

$$u_1^C(x_1,0) = \frac{-\partial_{x_2}}{2\pi}\int_S \log|x-y|\omega_0(y)\,dy = \frac{1}{4\pi}\int_S \partial_{y_2}\log|x-y|^2\omega_0(y)\,dy.$$

Integrating in y_2 over each quadrant and re-grouping the terms, we obtain

$$\frac{1}{2\pi}\left(\int_0^\pi \log\frac{(x_1-y_1)^2}{(x_1-y_1)^2+\pi^2}\,dy_1 - \int_{-\pi}^0 \log\frac{(x_1-y_1)^2}{(x_1-y_1)^2+\pi^2}\,dy_1\right) = \\ \frac{1}{\pi}\int_0^\pi \log\frac{x_1-y_1}{x_1+y_1}\,dy_1 + \frac{1}{2\pi}\int_0^\pi \log\frac{(x_1+y_1)^2+\pi^2}{(x_1-y_1)^2+\pi^2}\,dy_1.$$

The last term satisfies

$$\int_0^\pi \log\left(1+\frac{4x_1y_1}{(x_1-y_1)^2+\pi^2}\right)dy_1 \le Cx_1.$$

Let us split the first term into two parts. First,

$$\int_{2x_1}^\pi \log\left(1-\frac{2x_1}{y_1+x_1}\right)dy_1 = -\int_{2x_1}^\pi \frac{2x_1}{y_1+x_1}\,dy_1 + O(x_1) = 2x_1\log x_1 + O(x_1).$$

Second, making the substitution $y_1 = x_1 z$ in the remaining part we obtain

$$\int_0^{2x_1} \log\frac{|x_1-y_1|}{x_1+y_1}\,dy_1 = x_1\int_0^2 \log\frac{|1-z|}{|1+z|}\,dz = O(x_1).$$

Collecting all the estimates we arrive at (2.19). □

Since $u_2(x_1,0)\equiv 0$, a trajectory starting at a point $(x_1^0,0)$, with $x_1^0\in(0,\pi)$ is just an interval

$$\Phi_t((x_1^0,0)) \equiv (x_1(t),0),$$

moving towards the origin. If x_1^0 is sufficiently small, the component $x_1(t)$ will satisfy

$$x_1'(t) \le x_1(t)\log x_1(t),$$

and so

$$\frac{d}{dt}(\log x_1(t)) \le \log x_1(t),$$

thus

$$\log x_1(t) \le e^t \log x_1^0,$$

and

$$x_1(t) \le x_1(0)^{\exp(t)}. \tag{2.22}$$

This estimate has a consequence for the Hölder regularity of the trajectory map. Since the origin is a stationary point of the flow, the inverse flow map $\Phi_t^{-1}(x)$ can be Hölder continuous only with a decaying in time exponent (at most $\sim e^{-t}$). Of course, the direct flow map $\Phi_t(x)$ also has a similar property; to establish it one needs to look at characteristic lines moving along the vertical separatrix. This is exactly the regularity claimed in Theorem 2.5, and thus the Bahouri-Chemin example shows that it cannot be improved.

3. The 2D Euler equation: an upper bound on derivative growth

More details on material of this section can be found in [16, 37, 39, 44]. We now turn to classical solutions of the 2D Euler equation whose existence and uniqueness are provided by Theorem 2.6. We work in a setting of a compact smooth domain D, but the arguments of this section can be adapted to work on periodic solutions (i.e., $\mathbb{T}^2$) or whole plane $\mathbb{R}^2$. The question that interests us is how quickly can the derivatives of the solutions grow. Such bounds are implicit already in the work of Wolibner [59] and Hölder [32], and have been stated explicitly by Yudovich.

Theorem 3.1. *Assume that $\omega_0 \in C^1(\bar{D})$. Then the gradient of the solution $\omega(x,t)$ satisfies the following bound*

$$\frac{\|\nabla\omega(\cdot,t)\|_{L^\infty}}{\|\omega_0\|_{L^\infty}} \le \left(1 + \frac{\|\nabla\omega_0\|_{L^\infty}}{\|\omega_0\|_{L^\infty}}\right)^{C\exp(\|\omega_0\|_{L^\infty}t)} e^{\exp(C\|\omega_0\|_{L^\infty}t)-1} - 1 \tag{3.1}$$

for all $t \ge 0$.

This upper bound grows at a double exponential rate in time which is extremely fast. A similar double exponential in time upper bound can also be derived for higher order derivatives of vorticity. The occurrence of the double exponential is unusual. Such fast growth, if realized, would pose a formidable challenge in numerical simulations. Let us sketch an argument leading to the estimate (3.1). There are three essential ingredients.

1. The kinematics. Using the trajectories equation (2.2) and some simple estimates, one can derive the following inequality.

$$\exp\left(-\int_0^t \|\nabla u(\cdot,s)\|_{L^\infty}\,ds\right) \le \frac{|\Phi_t(x)-\Phi_t(y)|}{|x-y|} \le \exp\left(\int_0^t \|\nabla u(\cdot,s)\|_{L^\infty}\,ds\right). \tag{3.2}$$

Since this bound is two sided, it also applies to to the inverse map $\Phi_t^{-1}(x)$.

2. The vorticity conservation along trajectories. The formula (2.3) implies that

$$\|\nabla\omega(\cdot,t)\|_{L^\infty} \le \|\nabla\omega_0\|_{L^\infty}\sup_{x,y}\frac{|\Phi_t^{-1}(x)-\Phi_t^{-1}(y)|}{|x-y|}. \tag{3.3}$$

3. The Kato inequality.

$$\|\nabla u\|_{L^\infty} \le C(\alpha,D)\|\omega\|_{L^\infty}\left(1+\log\left(1+\frac{\|\nabla\omega\|_{L^\infty}}{\|\omega\|_{L^\infty}}\right)\right). \tag{3.4}$$

The way to think about this inequality is as follows. The derivatives of u can be expressed as second order derivatives of the stream function, $\partial^2_{x_ix_j}(-\Delta_D)^{-1}\omega$. Such expressions are called (double) Riesz transforms of ω. These are classical objects in Fourier analysis, and lead to Caldreon-Zygmund operators. Riesz transforms are bounded on L^p, $1 < p < \infty$, but not in L^∞ or L^1 (see e.g. [48]). The structure of the problem, however, requires an L^∞ bound and then we have to pay a logarithm of a higher order norm.

Given (3.2), (3.3), and (3.4), the estimate (3.1) follows from some algebraic manipulations and application of Gronwall inequality.

4. The 2D Euler equation: an example of double exponential growth

More details on material of this section can be found in [37, 39].

A natural question prompted by Theorem 3.1 is whether the double exponential upper bound on growth of derivatives of vorticity is sharp. A variety of examples with some growth in derivatives have been provided by a number of authors. Yudovich [61, 62] built first such examples with growth near the boundary using Lyapunov-type functionals, but without explicit growth rate bounds. Nadirashvili's [49] example is set in an annulus, and is based on using a perturbation of a stable background shear flow. The rate of growth in this example can be shown to be linear in time. Denisov [16] has constructed a periodic solution such that $\|\nabla\omega\|_{L^\infty}$ grows faster than linearly (in a certain average sense). In [17], Denisov has constructed examples with extremely strong (double exponential in time in a certain sense) bursts of growth in derivatives over finite time interval. The idea of Denisov's construction goes back to the singular cross example. Indeed, imagine that a smooth passive scalar $\psi(x,t)$ is advected by the singular cross flow u, that is,

$$\partial_t\psi + (u\cdot\nabla)\psi = 0. \tag{4.1}$$

Assume that the initial data ψ_0 is a C_0^∞ bump supported away from the origin and but nonzero on the $x_2 = 0$ separatrix for $x_1 \sim \delta > 0$, δ sufficiently small. Then $\psi(\Phi_t(\delta,0),t) = \psi_0(\delta) > 0$, while (2.22) shows that $\Phi_t(\delta,0) \le \delta^{\exp(t)}$. At the same time, $\psi(0,t) = 0$ since the origin is a stationary point of the singular cross flow. Together, these observations imply that

$$\|\nabla\psi(\cdot,t)\|_{L^\infty} \ge \psi_0(\delta)\delta^{-\exp(t)},$$

and is therefore growing at a double exponential rate. The 2D Euler equation for vorticity has the same form as (4.1), but of course it is not passive. Changes in ω affect u. Yet the idea of Denisov is to smooth out the singular cross at a very small scale (which depends on how long we would like to control the solution), and to place a perturbation close to the separatrix. In the end, one can mimic the effect of the singular cross flow on passive scalar small scale formation for a finite time, but then control is lost.

The purpose of this section is to present an example where double exponential growth in $\|\nabla\omega\|_{L^\infty}$ is maintained for all times, thus showing that the upper bound of Theorem 3.1 is in general qualitatively sharp [37].

Theorem 4.1. *Consider the two-dimensional Euler equation on a unit disk D. There exist smooth initial data ω_0 with $\|\nabla\omega_0\|_{L^\infty}/\|\omega_0\|_{L^\infty} > 1$ such that the corresponding solution $\omega(x,t)$ satisfies*

$$\frac{\|\nabla\omega(x,t)\|_{L^\infty}}{\|\omega_0\|_{L^\infty}} \ge \left(\frac{\|\nabla\omega_0\|_{L^\infty}}{\|\omega_0\|_{L^\infty}}\right)^{c\exp(c\|\omega_0\|_{L^\infty}t)} \tag{4.2}$$

for some $c > 0$ *and for all* $t \geq 0$.

The example can be extended to any smooth domain with an axis of symmetry [60].

From now on in this section, we will denote by D the unit disk in the plane. It will be convenient for us to take the system of coordinates centered at the lowest point of the disk, so that the center of the disk is at $(0,1)$. Our initial data $\omega_0(x)$ will be odd with respect to the vertical axis: $\omega_0(x_1, x_2) = -\omega_0(-x_1, x_2)$.

We will take smooth initial data $\omega_0(x)$ so that $\omega_0(x) \leq 0$ for $x_1 > 0$ (and so $\omega_0(x) \geq 0$ for $x_1 < 0$). This configuration makes the origin a hyperbolic fixed point of the flow; in particular, u_1 vanishes on the vertical axis. Let us analyze the Biot-Savart law we have for the disk to gain insight into the structure of the velocity field. The Dirichlet Green's function for the disk is given explicitly by $G_D(x,y) = -\frac{1}{2\pi}(\log|x-y| - \log|x-\bar{y}| - \log|y-e_2|)$, where with our choice of coordinates $\bar{y} = e_2 + (y-e_2)/|y-e_2|^2$, $e_2 = (0,1)$. Given the symmetry of ω, we have

$$u(x,t) = \nabla^\perp \int_D G_D(x,y)\omega(y,t)\,dy = -\frac{1}{2\pi}\nabla^\perp \int_{D^+} \log\left(\frac{|x-y||\tilde{x}-\bar{y}|}{|x-\bar{y}||\tilde{x}-y|}\right)\omega(y,t)\,dy, \tag{4.3}$$

where D^+ is the half disk where $x_1 \geq 0$, and $\tilde{x} = (-x_1, x_2)$. The following Lemma is crucial for the proof of Theorem 4.1. To state it, we need a bit more notation. Let us introduce notation $Q(x_1,x_2)$ for a region that is the intersection of D^+ and the quadrant $x_1 \leq y_1 < \infty$, $x_2 \leq y_2 < \infty$. Given $\pi/2 > \gamma > 0$, denote D_1^γ the intersection of D^+ with a sector $\pi/2 - \gamma \geq \phi \geq 0$, where ϕ is the usual angular variable. Similarly, define D_2^γ the intersection of D^+ with a sector $\pi/2 \geq \phi \geq \gamma$.

Lemma 4.2. *Fix the value of* γ, $\pi/2 > \gamma > 0$ *(later it will be convenient to take* γ *sufficiently small, in particular* $\gamma < \pi/4$*). Suppose that* $x \in D_1^\gamma$. *Then there exists* $\delta > 0$ *such that for all* $x \in D_1^\gamma$ *such that* $|x| \leq \delta$ *we have*

$$u_1(x_1,x_2,t) = \frac{4}{\pi}x_1 \int_{Q(x_1,x_2)} \frac{y_1y_2}{|y|^4}\omega(y,t)\,dy_1dy_2 + x_1B_1(x_1,x_2,t), \tag{4.4}$$

where $\|B_1(\cdot,t)\|_\infty \leq C(\gamma)\|\omega_0\|_{L^\infty}$.

If $x \in D_2^\gamma$ *is such that* $|x| \leq \delta$ *then we have*

$$u_2(x_1,x_2,t) = -\frac{4}{\pi}x_2 \int_{Q(x_1,x_2)} \frac{y_1y_2}{|y|^4}\omega(y,t)\,dy_1dy_2 + x_2B_2(x_1,x_2,t), \tag{4.5}$$

where $\|B_2(\cdot,t)\|_\infty \leq C(\gamma)\|\omega_0\|_{L^\infty}$.

The proof of the lemma is based on careful analysis of the Biot-Savart law; the details can be found in [37,39].

It will be convenient to denote

$$\Omega(x_1,x_2,t) = -\frac{4}{\pi}x_2 \int_{Q(x_1,x_2)} \frac{y_1y_2}{|y|^4}\omega(y,t)\,dy_1dy_2. \tag{4.6}$$

Now let us select the initial data as follows. Fix some small γ, and choose $\delta < 1$ so that the bounds of Lemma 4.2 hold. Note that in what follows, we can always make δ smaller if necessary. Take $\omega_0(x) = -1$ if $x_1 \geq \delta$, odd with respect to x_1, and satisfying $0 \geq \omega_0(x) \geq -1$ for $x \in D^+$.

Lemma 4.3. *Let the initial data ω_0 be as above. Suppose that $|x| \leq \delta$. Then, if δ is sufficiently small, we have*

$$\Omega(x_1, x_2, t) \geq c \log \delta^{-1} \tag{4.7}$$

for some universal constant $c > 0$. Here $\Omega(x_1, x_2, t)$ is given by (4.6).

Proof. We sketch the proof of this estimate leaving detailed computations to the reader. The key observation is that the trajectory map $\Phi_t(x)$ and its inverse are area preserving, while $\omega(x,t) = \omega_0(\Phi_t^{-1}(x))$. For this reason, for all times t, the area of the set $S_t \subset D^+$ where $-1 < \omega(x,t) < 0$ does not exceed 2δ; on the complement of S_t we have $\omega(x,t) = -1$. Given this observation, (4.4) and the formula (4.6), it is not hard to devise a lower bound estimate that will show (4.7). The singularity of the kernel in (4.6) would yield $\log |x|^{-1} \gtrsim \log \delta^{-1}$ if integrated against -1 over all $Q(x_1, x_2)$, and removing a set of measure $\leq 2\delta$ from the integration region will preserve the lower bound by $\log \delta^{-1}$. □

Now we will put one more requirement on the initial data. Given $0 < x_1' < x_1'' < 1$, we set

$$\mathcal{O}(x_1', x_1'') = \left\{(x_1, x_2) \in D^+ ,\ x_1' < x_1 < x_1'' ,\ x_2 < x_1\right\} . \tag{4.8}$$

We are going to take a sufficiently small $\epsilon < \delta$ and require in addition that $\omega_0(x) = -1$ for $x \in \mathcal{O}(\epsilon^{10}, \epsilon)$. We can find ω_0 satisfying this requirement such that $\|\nabla \omega_0\|_{L^\infty} \lesssim \epsilon^{-10}$.

Let us also define, for $0 < x_1 < 1$,

$$\underline{u}_1(x_1, t) = \min_{(x_1,x_2)\in D^+ ,\, x_2 \leq x_1} u_1(x_1, x_2, t) \tag{4.9}$$

and

$$\overline{u}_1(x_1, t) \quad = \max_{(x_1,x_2)\in D^+ ,\, x_2 \leq x_1} u_1(x_1, x_2, t)\, . \tag{4.10}$$

Since $\omega(x,t)$ and $u(x,t)$ are smooth by Theorem 2.6, these functions are locally Lipschitz in x_1 on $[0, 1)$, with the Lipschitz constants being locally bounded in time. Hence, we can uniquely define $a(t)$ by

$$a' = \overline{u}_1(a, t)\, , \quad a(0) = \epsilon^{10}\, , \tag{4.11}$$

and $b(t)$ by

$$b' = \underline{u}_1(b, t)\, , \quad b(0) = \epsilon\, . \tag{4.12}$$

We set

$$\mathcal{O}_t = \mathcal{O}(a(t), b(t)) \tag{4.13}$$

note that $\mathcal{O}_0$ is exactly the set where we set $\omega_0 = -1$ (in addition to the $x_1 \geq \delta$ region). The next key observation is

Lemma 4.4. *We have $\omega(x,t) = -1$ for $x \in \mathcal{O}_t$ for all $t \geq 0$.*

Note that for what we know so far, $\mathcal{O}_t$ may become empty at some point in time. We will see later that this is not the case.

Proof. Here is the sketch of the argument. Note that due to Lemma 4.3, if δ is chosen sufficiently small, then $\mathcal{O}_t$ will lie in the region $x_1 \leq \delta$ for all times and thus the estimates of Lemma 4.2 will continue to apply for all times. The main idea is that given any point $y \in \mathcal{O}_t$, we have $y = \Phi_t(x)$ with $x \in \mathcal{O}_0$. If we can show that, then the lemma is proved by (2.3). Suppose that this is not true, and some trajectory $\Phi_t(x)$ for $x \notin \mathcal{O}_0$ ends up inside $\mathcal{O}_t$. This trajectory cannot enter through the boundary ∂D due to the boundary condition. It also could not have entered through the left and right sides of the region $\mathcal{O}_s$ due to definitions of a, b, $\overline{u}$ and $\underline{u}$. It remains to consider the diagonal $x_1 = x_2$. However, by Lemma 4.2 and Lemma 4.3, we have

$$\frac{c\log\delta^{-1} - C}{c\log\delta^{-1} + C} \leq \frac{-u_1(x_1,x_1,t)}{u_2(x_1,x_1,t)} \leq \frac{c\log\delta^{-1} + C}{c\log\delta^{-1} - C}.$$

If δ is sufficiently small, this shows that any trajectory on the diagonal part of the boundary of $\mathcal{O}_t$ is always moving out of $\mathcal{O}_t$, and hence no trajectory could have entered $\mathcal{O}_t$ through the diagonal. □

Now we are going to complete the construction of the example.

Proof of Theorem 4.1. To get double exponential growth of the derivatives, we need a genuinely nonlinear argument; it is not sufficient to show that $\Omega(x,t)$ is large for all times as we did in Lemma 4.3. Instead, we will show that $\Omega(x,t)$ grows due to region $\mathcal{O}_t$ approaching the origin and remaining sufficiently large. Lemma 4.2 yields

$$\underline{u}_1(b(t),t) \geq -b(t)\,\Omega(b(t),x_2(t),t) - C\,b(t),$$

for some $0 \leq x_2(t) \leq b(t)$ and a constant C that may depend only on γ. A simple calculation shows that, for any $0 \leq x_2 \leq b(t)$ we have

$$\Omega(b(t),x_2,t) \leq \Omega(b(t),b(t),t) + C.$$

Thus, we get

$$\underline{u}_1(b(t),t) \geq -b(t)\,\Omega(b(t),b(t),t) - C\,b(t), \tag{4.14}$$

with C a new universal constant; below the constant C may change from step to step. In the same vein, for suitable $\tilde{x}_2(t)$ with $0 \leq \tilde{x}_2(t) \leq a(t)$, we have

$$\overline{u}_1(a(t),t) \leq -a(t)\,\Omega(a(t),\tilde{x}_2(t),t) + Ca(t) \leq -a(t)\,\Omega(a(t),0,t) + Ca(t).$$

A key observation is that

$$\Omega(a(t),0,t) \geq -\frac{4}{\pi}\int_{\mathcal{O}_t} \frac{y_1y_2}{|y|^4}\omega(t,y)\,dy_1dy_2 + \Omega(b(t),b(t),t).$$

Since $\omega(y,t) = -1$ on $\mathcal{O}_t$, we have

$$-\int_{\mathcal{O}_t} \frac{y_1y_2}{|y|^4}\omega(t,y)\,dy_1dy_2 \geq \int_{\pi/8}^{\pi/4}\int_{a(t)/\cos\phi}^{b(t)/\cos\phi} \frac{\sin 2\phi}{2r}\,drd\phi > \frac{1}{8}(-\log a(t) + \log b(t)).$$

Therefore

$$\overline{u}_1(a(t),t) \leq -\,a(t)\left(\frac{1}{2\pi}(-\log a(t) + \log b(t)) + \Omega(b(t),b(t),t)\right) + Ca(t). \tag{4.15}$$

It follows from (4.14) and (4.15) that

$$\frac{d}{dt}\left(\log a(t) - \log b(t)\right) \leq \frac{1}{2\pi}\left(\log a(t) - \log b(t)\right) + C. \tag{4.16}$$

From (4.16), the Gronwall lemma leads to

$$\log a(t) - \log b(t) \leq \log\left(a(0)/b(0)\right)\exp(t/2\pi) + C\exp(t/2\pi) \leq (9\log\epsilon + C)\exp(t/2\pi). \tag{4.17}$$

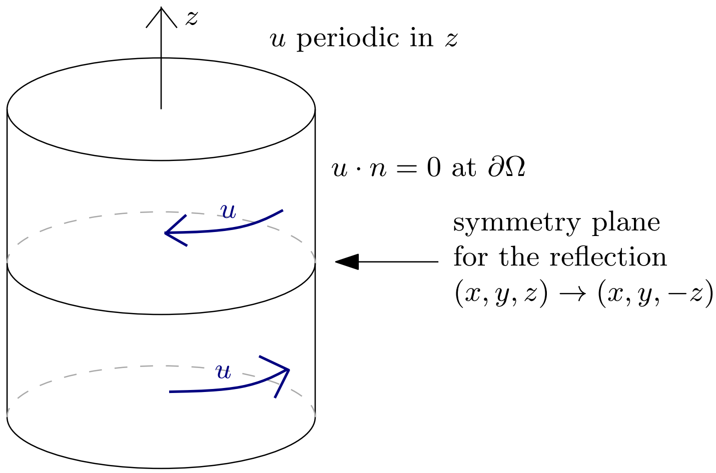

Figure 1. The initial data for Hou-Luo scenario

We should choose our ϵ so that $-\log\epsilon$ is larger than the constant C that appears in (4.17). In this case, we obtain from (4.17) that

$$\log a(t) \leq 8\exp(t/2\pi)\log\epsilon,$$

and so

$$a(t) \leq \epsilon^{8\exp(t/2\pi)}.$$

Note that by the definition of $a(t)$, the first coordinate of the characteristic that originates at the point on ∂D near the origin with $x_1 = \epsilon^{10}$ does not exceed $a(t)$. To arrive at (4.2), it remains to note that we chose ω_0 so that $\|\nabla\omega_0\|_{L^\infty} \lesssim \epsilon^{-10}$. □

5. The Hou-Luo scenario for the 3D Euler equation

More information on the material of this section can be found in [43,44]. The global regularity vs finite time blow up question for smooth solutions of the 3D Euler equation is open. There has been much work on local well-posedness, on conditional regularity criteria, as well as on search for singular scenario. How would finite time blow up manifest itself? In general, any loss of regularity by smooth solution qualifies. However, from many conditional criteria one can infer certain minimal conditions needed for blow up. Perhaps the best known and one of the earliest such conditions was proved by Beale, Kato and Majda [2,44]. It states that at the singularity formation time T, one must have

$$\lim_{t\to T}\int_0^t \|\omega(\cdot,s)\|_{L^\infty}\,ds = \infty.$$

A few years ago, Hou and Luo [43] have performed an in-depth numerical simulation, identifying a promising singularity formation scenario. The scenario is axi-symmetric (that is, there is no dependence on the angular variable ϕ in the cylindrical coordinates) and odd with respect to $z = 0$ plane. Very fast vorticity growth is observed at a ring of hyperbolic stagnation points of the flow located on the boundary of a cylinder. In fact, the geometry of the scenario is similar to that of the double exponential growth example for the 2D Euler we discussed in the previous section; the paper [37] has been inspired by the numerical simulations of [43].

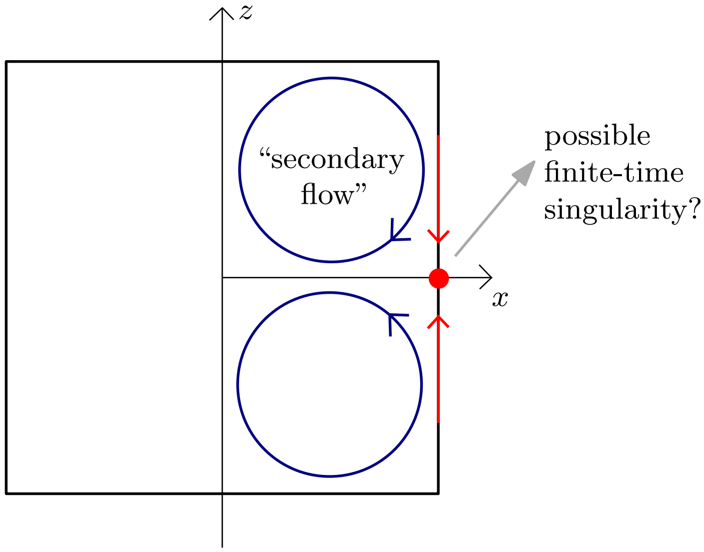

FIGURE 2. The secondary flows in fixed ϕ section

One of the standard forms of the 3D axi-symmetric Euler equations in the usual cylindrical coordinates (r, ϕ, z) is (see e.g. [44] for more details)

$$\partial_t \left(\frac{\omega^\phi}{r}\right) + u^r \partial_r \left(\frac{\omega^\phi}{r}\right) + u^z \partial_z \left(\frac{\omega^\phi}{r}\right) = \partial_z \left(\frac{(ru^\phi)^2}{r^4}\right) \tag{5.1a}$$

$$\partial_t (ru^\phi) + u^r \partial_r (ru^\phi) + u^z \partial_z (ru^\phi) = 0\,, \tag{5.1b}$$

with the understanding that u^r, u^z are given from ω^ϕ via the Biot-Savart law which takes form

$$u^r = -\frac{\partial_z \psi}{r}, \;\; u^z = \frac{\partial_r \psi}{r}, \;\; L\psi = \frac{\omega^\phi}{r}, \;\; L\psi = -\frac{1}{r}\partial_r \left(\frac{1}{r}\partial_r \psi\right) - \frac{1}{r^2}\partial^2_{zz}\psi.$$

The initial data for the Hou-Luo scenario, shown schematically on Figure 1, has $\omega^\phi = 0$ and only the swirl u^ϕ is non-zero. From (5.1), it is clear that the swirl will spontaneously generate toroidal rolls corresponding to non-zero ω^ϕ. These are the so-called "secondary flows", [51]; their effect on river flows was studied by Einstein [19]. Thus the initial condition leads to the (schematic) picture in the xz–plane shown on Figure 2, in which we also indicate the point where a conceivable finite-time singularity (or at least an extremely strong growth of vorticity) is observed numerically. In the three-dimensional picture, the points with very fast growth form a ring on the boundary of the cylinder.

A similar scenario can be considered for the 2D inviscid Boussinesq system in a half-space $\mathbb{R}^+ = \{(x_1, x_2) \in \mathbb{R} \times (0, \infty)\}$ (or in a flat half-cylinder $\mathbf{S}^1 \times (0, \infty)$), which we will write in the vorticity form:

$$\partial_t \omega + (u \cdot \nabla)\omega = \partial_{x_1}\theta \tag{5.2a}$$

$$\partial_t \theta + (u \cdot \nabla)\theta = 0\,. \tag{5.2b}$$

Here $u = (u_1, u_2)$ is obtained from ω by the usual Biot-Savart law $u = \nabla^\perp(-\Delta)^{-1}\omega$, with appropriate boundary conditions on Δ, and θ represents fluid temperature or density.

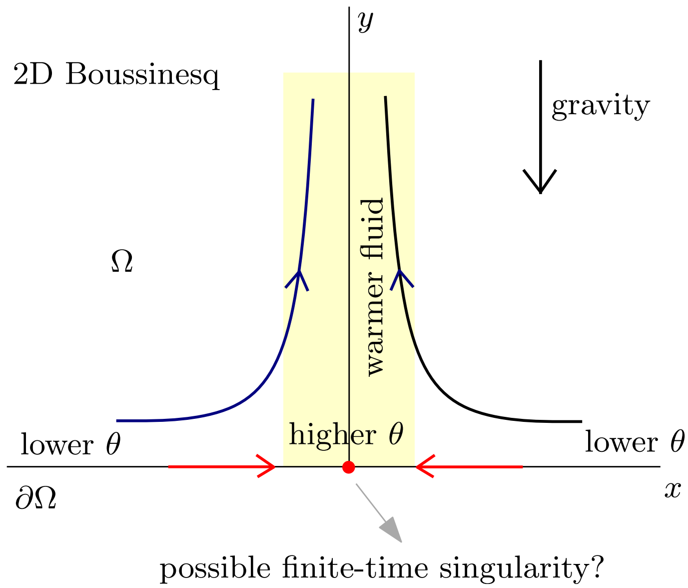

FIGURE 3. The 2D Boussineq singularity scenario

It is well-known (see [44]) that this system has properties similar to the 3D axi-symmetric Euler (5.1), at least away from the symmetry axis. Indeed, comparing (5.1) with (5.2), we see that θ essentially plays the role of the square of the swirl component ru^ϕ of the velocity field u, and ω replaces ω^ϕ/r. The real difference between the two systems only emerges near the axis of rotation, where factors of r can conceivably change the nature of dynamics. For the purpose of comparison with the axi-symmetric flow, the last picture should be rotated by $\pi/2$, after which it resembles the picture relevant for (5.2), see Figures 2 and 3. The system (5.2) has an advantage of being simpler looking and easier to think about while very likely preserving all the essential features. Of course, the question of global regularity vs finite time blow up is also open for the 2D inviscid Boussinesq; in fact it appears on the list of "eleven great problems of mathematical hydrodynamics" by Yudovich [63].

In both the 3D axi-symmetric Euler case and in the 2D Boussinesq system case the best chance for possible singularity formation seems to be at the points of symmetry located at the boundary, which numerical simulations suggest are fixed hyperbolic points of the flow. So far there is no proof of singularity formation for smooth solutions in the Hou-Luo scenario, but a number of models have been proposed (e.g. [9, 10, 18, 31, 33, 41, 42]). All these models suggest finite time blow up. In the next section, we will take a look at one of the simpler ones that provides a qualitative insight into the nature of possible nonlinear feedback loop leading to singularity.

In addition, there is recent and very interesting work by Elgindi and Elgindi and Jeong [21–23] and [7] where the initial data is taken to be singular, to a varying degree, in a scenario very similar to that of Hou-Luo and involving stationary hyperbolic points of the flow. Then finite time blow up is shown in a sense of the solution becoming more singular than the initial data. In [21, 22] the domain needs to have a corner (for the 2D Boussinesq, and a wedge for the 3D Euler), and the initial vorticty is just L^∞, but becomes unbounded in finite time. The work [23] is set in the whole space, and the initial vorticity is Hölder continuous, leading to a solution satisfying

$$\lim_{t\to 1}\int_0^t \|\omega(\cdot,t)\|_{L^\infty}\,dt = \infty.$$

The paper [7] builds on [23] and [8] and proves finite time blow up for solutions with C^α initial vorticity and $C^{1,\alpha}$ density (respectively, swirl) in the Hou-Luo scenario.

6. Singularities and turbulence

In this section, we take a step back to look at the big picture. The material in this section is motivational and largely informal. Most of the statements and problems mentioned here are either heuristic or remain wide open. One of the incentives in trying to understand and describe small scale and possible singularity formation in solutions to equations of fluid mechanics is the connection to turbulence. Turbulence is familiar to all of us from bumpy airplane ride or fluctuations we feel in strong wind. It is a ubiquitous feature of intense fluid motion, and plays a role in a wide range of processes in nature: drag effects for cars and airplanes, efficiency of internal combustion engines, mixing crucial for survival of marine animals, or even evolution of temperature inside Earth [58]! Nevertheless, turbulence remains relatively poorly understood: Richard Feynman has called it the greatest unsolved problem of classical physics fifty years ago, and not much has changed since. This situation is not for the lack of trying: a number of heuristic theories have been proposed by Prandtl, von Kármán, Richardson, Taylor, Heisenberg, Kolmogorov, Onsager, Kraichnan, and others, see e.g. [26] for review. These phenomenological theories have been quite successful in predicting some of the properties of turbulent flows, but deeper understanding and in particular rigorous connection to the partial differential equations of fluid mechanics have not been established. Among these predictions, the one most consistent with experiments and reported at least as early as Dryden's wind tunnel experiments in 1943, is Kolmogorov's "zeroth law of turbulence" which postulates *anomalous dissipation of energy*, that is, non-vanishing of the rate of dissipation of kinetic energy of turbulent fluctuations per unit mass, in the limit of zero viscosity. Let u^ν be solutions of the 3D Navier-Stokes equations with viscosity ν (in the non-dimensional form, ν is equal to the inverse of the Reynolds number, $Re = \frac{UL}{\sigma}$, where σ is the actual viscosity and U, L typical velocity and length scales):

$$\partial_t u^\nu + (u^\nu\cdot\nabla)u^\nu - \nu\Delta u^\nu = \nabla p^\nu + f, \quad \nabla\cdot u^\nu = 0,$$

where f is some spatially regular forcing. Notice that $\nu\int|\nabla u^\nu|^2\,dx$ is just an instantaneous rate of energy dissipation. Then the zeroth law states that

$$\lim_{\nu\to 0}\nu\langle|\nabla u^\nu(x,t)|^2\rangle > 0, \tag{6.1}$$

where $\langle\cdot\rangle$ represents a suitable ensemble or space-time average. On the other hand, one may expect that as $\nu\to 0$, u^ν converges to the solution u of the incompressible 3D Euler equation. This is far from clear, especially when there are boundaries. But if we accept this as a reasonable assumption, and the limiting solution is smooth, then the limit of the enstropy $\int|\nabla u^\nu|^2\,dx$ should equal $\int|\nabla u|^2\,dx < \infty$, and so (6.1) cannot hold. Therefore, if the zeroth law of turbulence is mathematically valid, it is intimately linked with singularity formation in the solutions of the Euler (and possibly Navier-Stokes) equation. In fact, the zeroth law has been rigorously proved in just one PDE setting: for stochastically forced Burgers equation [20].

In this case, the underlying singularities are well understood shocks, and this is a key aspect that makes the problem approachable.

The set up of the Hou-Luo scenario seems to be rather special, but there are indications that hyperbolic point geometry plays an important role in extreme dissipation regions in turbulent fluid flows. In a paper [53], the authors describe a physical experiment where they study turbulence. The geometry of the experiment is very similar to the Hou-Luo setting: the flows are confined to a cylinder and are statistically axi-symmetric (of course, in any real flow the exact axial symmetry breaks down spontaneously). Using particle image velocimetry techniques, they are able to capture the structure of fluid flow in the regions of "extreme inertial dissipation events". These are regions where the dissipation rate is anomalously large, essentially the regions that would facilitate the zeroth law as viscosity decreases. There are four different geometric scenarios documented in [53], and by far the most common is the one where vorticity growth happens at the front between colliding masses of fluid with different directions of the velocity and hyperbolic point geometry. In this sense, the Hou-Luo scenario may be thought of as an idealized blueprint of what appears to be a common small scale formation mechanism.

In recent years, there have been other works on singularity formation in equations of fluid mechanics, in particular by Terry Tao [56, 57]. In these papers, finite time blow up is proved for modified Euler and Navier-Stokes equations; the modifications involve suitable averaging or changes in coupling of the Fourier modes. The philosophy of these examples is different from Hou-Luo scenario and involves instead a self-similar picture of energy transition to smaller and smaller scales. Inspired by these ideas, the paper [4] has outlined a specific physical mechanism that could be behind such self-similar cascades: repeated flattening of vortex tubes into sheets and breakup of the sheets into tubes. There are some numerical simulations, however (see e.g. [47] where further references can be found), that suggest that this process is quite complex and it is not clear whether some sort of approximate self-similarity can be traced over smaller and smaller scales.

7. One-dimensional models of the Hou-Luo scenario

More details on the results discussed in this section can be found in [9, 10, 43]. A one-dimensional model of the Hou-Luo scenario was formulated already in [43]. This model is given by

$$\begin{aligned} \partial_t \omega + u \partial_x \omega &= \partial_x \theta, \\ \partial_t \theta + u \partial_x \theta &= 0, \;\; u_x = H\omega. \end{aligned} \tag{7.1}$$

Here H is the Hilbert transform, and the setting can be either periodic or the entire axis with some decay of the initial data. The model (7.1) can be thought of as an effective equation on the $x_2 = 0$ axis in the Boussinesq case (see (5.2) and Figure 3) or on the boundary of the cylinder in the 3D axi-symmetric Euler case. The model can be derived from the full equations under assumption that $\omega(x, t)$ is concentrated in a boundary layer of width a near $x_2 = 0$ axis and is independent of x_2, that is $\omega(x_1, x_2, t) = \omega(x_1, t)\chi_{[0,a]}(x_2)$. Such assumption is necessary to close the system and reduces the half-plane Biot-Savart law to $u_x = H\omega$ in the main order; the parameter a enters into the additional term that is non-singular and is dropped from (7.1). See [43], [10] for more details. We will call the system (7.1) the Hou-Luo model.

The Hou-Luo model is still fully nonlocal. A further simplification was proposed in [9], where the Biot-Savart law has been replaced with

$$u(x,t) = -x \int_x^1 \frac{\omega(y,t)}{y}\, dy. \tag{7.2}$$

Here the most natural setting is on an interval $[0,1]$ with smooth initial data supported away from the endpoints. For simplicity we set the Biot-Savart law so that blow up at zero happens for positive vorticity. The law (7.2) is motivated by the velocity representation in Lemma 4.2 above, as it is the simplest one dimensional analog of such representation. This law is "almost local" - if one divides u by x and differentiates, one gets local expression. We will call the model (7.2) the CKY model. The law (7.2) models the situation where ω is odd in x_1, and with this additional assumption one can show that it is not too different from the relation $u_x = H\omega$ in the Hou-Luo model.

Both Hou-Luo and CKY models are locally well-posed in reasonable spaces, and in both cases possibility of finite time blow up has been proved in [9] and [10] respectively. Here we sketch the arguments showing singularity formation in the CKY model [9]. In this section, let us denote

$$\Omega(x,t) = \int_x^1 \frac{\omega(y,t)}{y}\, dy. \tag{7.3}$$

The first step is the following

Lemma 7.1. *Along the trajectories $\Phi_t(x)$, we have*

$$\frac{d}{dt}\Omega(\Phi_t(x),t) = \int_{\Phi_t(x)}^1 \frac{\omega(y,t)^2}{y} dy + \int_{\Phi_t(x)}^1 \frac{\partial_x \theta(y,t)}{y} dy. \tag{7.4}$$

The proof of this lemma is a direct computation taking advantage of (7.1), (7.2), and integration by parts. A key observation is the positivity of the first term in the right hand side of (7.4).

Consider now $\psi(x,t) := \log \Phi_t(x)^{-1}$. From (7.2), we have that

$$\partial_t \psi(x,t) = \Omega(\Phi_t(x),t). \tag{7.5}$$

On the other hand, from Lemma 7.1, we have that

$$\frac{d}{dt}\Omega(\Phi_t(x),t) \geq \int_{\Phi_t(x)}^1 \frac{\partial_x \theta(y,t)}{y} dy. \tag{7.6}$$

Let us trace a trajectory that originates at some point in the support of θ where $\partial_x \theta$ is not zero. As the flow pushes the vorticity support towards the origin, we expect that the front of the graph of θ will become very steep. Then morally, we can think of the integral on the right hand side of (7.6) as

$$\int_{\Phi_t(x)}^1 \frac{\partial_x \theta(y,t)}{y} dy \sim \Phi_t(x)^{-1} = e^{\psi(x,t)},$$

as most of the variation of θ will be supported close to $\Phi_t(x)$. If we accept this heuristic argument for a moment, we get a system of differential inequalities

$$\partial_t \psi(x,t) = \Omega(\Phi_t(x),t), \;\; \partial_t \Omega(\Phi_t(x),t) \gtrsim e^{\psi(x,t)}$$

for which it is not hard to prove finite time blow up. Such blow up corresponds to a trajectory carrying some positive value of the density arriving at the origin at a finite time $T < \infty$, which one can show only happens if $\int_0^T \|\omega(\cdot,t)\|_{L^\infty}\,dt = \infty$.

A more careful argument to establish blow up uses a cascade of trajectories corresponding to a sequence of initial points with larger and larger values of θ_0, and iterative estimates. The details can be found in [9].

8. The modified SQG equation: singularity formation in patches

More details regarding material of this section can be found in [34, 38, 40]. Note that the 2D Euler equation is just the 2D inviscid Boussinesq system with $\theta \equiv 0$. It is tempting to try to extend the insight and techniques used in the proof of Theorem 4.1 to analysis of the Hou-Luo scenario. There are several issues that arise in such an attempt. Perhaps the most significant one is that the vorticity may no longer be bounded, so the result of Lemma 4.2 giving fairly precise control over fluid velocity near the origin is not available. The kernel in the Biot-Savart law is not sign definite, and growth of vorticity may conceivably make the contributions of the regions that in Lemma 4.2 end up in the regular Lipschitz term no longer relatively small. This might destroy the hyperbolic structure of the flow and sabotage singularity formation. The available evidence suggests that singularity formation likely holds - the numerical computations of Hou and Luo are very detailed and precise, all the models considered so far suggest blow up, and so does the work of Elgindi and Jeong [21–23]. Yet there are counter arguments to all these points. Any numerical simulation has a limit; the models of the Hou-Luo scenario make simplifying assumptions on the Biot-Savart law and other aspects of the problem; and the works on rough initial data do not apply to smooth initial data.

In this section, we discuss a blow up example in a different setting, where nevertheless some of the technical issues are similar. In particular, we will see that the term pushing towards singularity has the same order as the term opposing it (in contrast to Lemma 4.2 where we could isolate a relatively simple dominant main term). This setting is patch solutions to modified surface quasi-geostrophic (SQG) equation.

The SQG equation is similar to the 2D Euler equation in vorticity form, but is more singular:

$$\partial_t\omega + (u\cdot\nabla)\omega = 0, \;\; u = \nabla^\perp(-\Delta)^{-1+\alpha}\omega, \;\; \alpha = 1/2, \;\; \omega(x,0) = \omega_0(x). \tag{8.1}$$

The value $\alpha = 0$ in (8.1) corresponds to the 2D Euler equation, while $0 < \alpha < \frac{1}{2}$ is the so-called modified SQG range. The SQG and modified SQG equations come from atmospheric science. They model evolution of temperature near the surface of a planet and can be derived by formal asymptotic analysis from a larger system of rotating 3D Navier-Stokes equations coupled with temperature equation through buoyancy force [30, 39, 45, 50]. In mathematical literature, the SQG equation was first considered by Constantin, Majda and Tabak [12], where a parallel between the structure of the SQG equation and the 3D Euler equation was drawn. A singularity formation scenario, a closing front, has been proposed in [12], but it was later proved to be impossible under certain additional assumptions in [13, 14]. The SQG and modified SQG equations are perhaps simplest looking equations of fluid mechanics for which the question of global regularity vs finite time blow up remains open.

The equation (8.1) can be considered with smooth initial data, but another important class of initial data is patches, where $\theta_0(x)$ equals linear combination of characteristic functions of some disjoint domains $\Omega_j(0)$. The resulting evolution yields time dependent regions $\Omega_j(t)$. The regularity question in this context addresses the regularity class of the boundaries $\partial\Omega_j(t)$ and lack of self-intersection or contact between different components $\Omega_j(t)$. Existence and uniqueness of patch solution for 2D Euler equation follows from Yudovich theory. The global regularity question has been settled affirmatively by Chemin [6] (Bertozzi and Constantin [3] provided a different proof). For the SQG and modified SQG equations patch dynamics is harder to set up. Local well-posedness has been shown by Rodrigo in C^∞ class [52] and by Gancedo in Sobolev spaces [27] in the whole plane setting. Numerical simulations by Cordoba, Fontelos, Mancho and Rodrigo [15] and by Dritschel and Scott [54, 55] suggest that finite time singularities are possible. There are different scenarios involving boundaries touching and forming corners [15,55] and self-similar cascade of filaments [54], but rigorous understanding of this phenomena remains missing.

We will discuss modified SQG and Euler patches in a half-plane. The Bio-Savart law for the patch evolution on the half-plane $D := \mathbb{R} \times \mathbb{R}^+$ is

$$u = \nabla^\perp(-\Delta_D)^{-1+\alpha}\omega,$$

with Δ_D being the Dirichlet Laplacian on D, which can also be written as

$$u(x,t) := \int_D \left(\frac{(x-y)^\perp}{|x-y|^{2+2\alpha}} - \frac{(x-\bar{y})^\perp}{|x-\bar{y}|^{2+2\alpha}} \right) \omega(y,t)dy. \tag{8.2}$$

Note that u is divergence free and tangential to the boundary. A traditional approach to the 2D Euler ($\alpha = 0$) vortex patch evolution, going back to Yudovich (see [46] for an exposition) is via the corresponding flow map. The active scalar ω is advected by u from (8.2) via

$$\omega(x,t) = \omega\left(\Phi_t^{-1}(x), 0\right), \tag{8.3}$$

where

$$\frac{d}{dt}\Phi_t(x) = u\left(\Phi_t(x), t\right) \qquad \text{and} \qquad \Phi_0(x) = x. \tag{8.4}$$

The initial condition ω_0 for (8.2)-(8.4) is patch-like,

$$\omega_0 = \sum_{k=1}^N \theta_k \chi_{\Omega_k(0)}, \tag{8.5}$$

with $\theta_1, \dots, \theta_N \neq 0$ and $\Omega_1(0), \dots, \Omega_N(0) \subseteq D$ bounded open sets, whose closures $\overline{\Omega_k(0)}$ are pairwise disjoint and whose boundaries $\partial\Omega_k(0)$ are simple closed curves of given regularity.

One reason the Yudovich theory works for the 2D Euler equations is that for ω which is (uniformly in time) in $L^1 \cap L^\infty$, the velocity field u given by (8.2) with $\alpha = 0$ is log-Lipschitz in space, and the flow map Φ_t is everywhere well-defined as discussed in Section 2. But when ω is a patch solution and $\alpha > 0$, the flow u from (8.2) is smooth away from the patch boundaries $\partial\Omega_k(t)$ but is only $1-\alpha$ Hölder continuous near $\partial\Omega_k(t)$, which is exactly where one needs to use the flow map. This creates significant technical difficulties in proving local well-posedness of patch evolution in some reasonable functional space. A naive intuition on why patch evolution can be locally well-posed for $\alpha > 0$ without boundaries is that one can show that the below-Lipschitz loss of regularity only affects the tangential component of the fluid velocity at patch boundary. The normal to patch component, that intuitively should determine the evolution of the patch, retains stronger regularity.

In presence of boundaries, the problem is even harder. Intuitively, one reason for the difficulties can be explained as follows. In the simplest case of the half-plane the reflection principle implies that the boundary can be replaced by a reflected patch (or patches) of the opposite sign. If the patch is touching the boundary, then the reflected and original patch are touching each other, and the low regularity tangential component of the velocity field generated by the reflected patch has strong influence on the boundary of the original patch near touch points. Even in the 2D Euler case, the global regularity for patches in general domains with boundaries remained open until very recently [35]. In the half-plane, a global regularity result has been established earlier in [38]:

Theorem 8.1. *Let $\alpha = 0$ and $\gamma \in (0, 1]$. Then for each $C^{1,\gamma}$ patch-like initial data ω_0, there exists a unique global $C^{1,\gamma}$ patch solution ω to* (8.3)*,* (8.2)*,* (8.4) *with $\omega(\cdot, 0) = \omega_0$.*

In the case $\alpha > 0$ with boundary, even local well-posedness results are highly non-trivial. The following result has been proved in [40] for the half-plane.

Theorem 8.2. *If $\alpha \in (0, \frac{1}{24})$, then for each H^3 patch-like initial data ω_0, there exists a unique local H^3 patch solution ω with $\omega(\cdot, 0) = \omega_0$. Moreover, if the maximal time T_ω of existence of ω is finite, then at T_ω a singularity forms: either two patches touch, or a patch boundary touches itself or loses H^3 regularity.*

On the other hand, in [38], it was proved that for any $\frac{1}{24} > \alpha > 0$, there exist patch-like initial data leading to finite time blow up.

Theorem 8.3. *Let $\alpha \in (0, \frac{1}{24})$. Then there are H^3 patch-like initial data ω_0 for which the unique local H^3 patch solution ω with $\omega(\cdot, 0) = \omega_0$ becomes singular in finite time (i.e., its maximal time of existence T_ω is finite).*

Together, Theorems 8.1 and 8.3 give rigorous meaning to calling the 2D Euler equation critical. In the half-plane patch framework $\alpha = 0$ is the exact threshold for phase transition from global regularity to possibility of finite time blow up.

Recently, the local well-posedness result of Theorem 8.2 and the finite time blow up example of Theorem 8.3 have been extended to $0 < \alpha < 1/3$ for H^2 patches in [28].

In what follows, we will sketch the proof of the blow up Theorem 8.3. Full details can be found in [38]. Let us describe the initial data set up. Denote $\Omega_1 := (\varepsilon, 4) \times (0, 4)$, $\Omega_2 := (2\varepsilon, 3) \times (0, 3)$, and let $\Omega_0 \subseteq D^+ \equiv \mathbb{R}^+ \times \mathbb{R}^+$ be an open set whose boundary is a smooth simple closed curve and which satisfies $\Omega_2 \subseteq \Omega_0 \subseteq \Omega_1$. Here ϵ is a small parameter depending on α that will be chosen later.

Let $\omega(x, t)$ be the unique H^3 patch solution corresponding to the initial data

$$\omega(x, 0) := \chi_{\Omega_0}(x) - \chi_{\tilde{\Omega}_0}(x) \tag{8.6}$$

with maximal time of existence $T_\omega > 0$. Here, $\tilde{\Omega}_0$ is the reflection of Ω_0 with respect to the x_2-axis. Then

$$\omega(x, t) = \chi_{\Omega(t)}(x) - \chi_{\tilde{\Omega}(t)}(x) \tag{8.7}$$

for $t \in [0, T_\omega)$, with $\Omega(t) := \Phi_t(\Omega_0)$. It can be seen from (8.2) that the rightmost point of the left patch on the x_1-axis and the leftmost point of the right patch on the x_1-axis will move toward each other. In the case of the 2D Euler equations $\alpha = 0$, Theorem 8.1 shows that the two points never reach the origin. When $\alpha > 0$ is small, however, it is possible to control

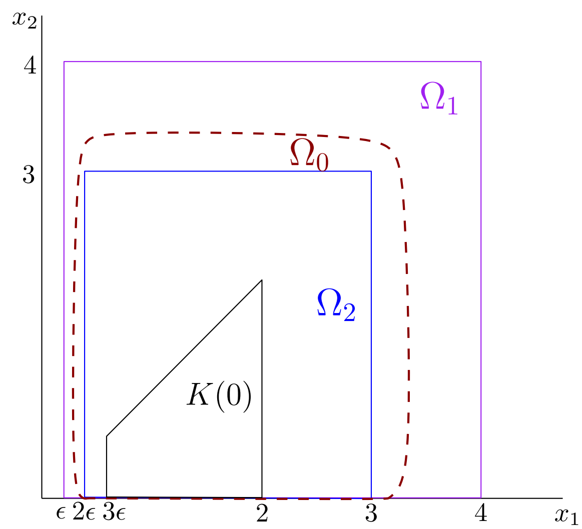

FIGURE 4. The domains $\Omega_1, \Omega_2, \Omega_0$, and $K(0)$ (with $\omega_0 = \chi_{\Omega_0} - \chi_{\tilde{\Omega}_0}$).

the evolution sufficiently well to show that — unless the solution develops another singularity earlier — both points will reach the origin in a finite time. The argument yielding such control is fairly subtle, and the estimates only work for sufficiently small α, even though one would expect singularity formation to persist for more singular equations. This situation is not uncommon in the field: there is plenty of examples with the infinite in time growth of derivatives for the smooth solutions of 2D Euler equation, while until very recently none were available for the more singular SQG equation - this will be discussed in the Section 9 below.

To show finite time blow up, we will deploy a barrier argument. Define

$$K(t) := \{x \in D^+ \,:\, x_1 \in (X(t), 2) \text{ and } x_2 \in (0, x_1)\} \tag{8.8}$$

for $t \in [0, T]$, with $X(0) = 3\epsilon$. Clearly, $K(0) \subset \Omega(0)$. Set the evolution of the barrier by

$$X'(t) = -\frac{1}{100\alpha} X(t)^{1-2\alpha}. \tag{8.9}$$

Then $X(T) = 0$ for $T = 50(3\epsilon)^{2\alpha}$. So if we can show that $K(t)$ stays inside $\Omega(t)$ while the patch solution stays regular, then we obtain that singularity must form by time T : the different patch components will touch at the origin by this time unless regularity is lost before that.

The key step in the proof involves estimates of the velocity near origin. In particular, u_1 needs to be sufficiently negative to exceed the barrier speed (8.9); u_2 needs to be sufficiently positive in order to ensure that $\Omega(t)$ cannot cross the barrier along its diagonal part. Note that it suffices to consider the part of the barrier that is very close to the origin, on the order $\sim \epsilon^{2\alpha}$. Indeed, the time T of barrier arrival at the origin has this order, and the fluid velocity satisfies uniform L^∞ bound that follows by a simple estimate which uses only $\alpha < 1/2$. Thus the patch $\Omega(t)$ has no time to reach more distant boundary points of the barrier before formation of singularity.

Let us focus on the estimates for u_1. For $y = (y_1, y_2) \in \bar{D}^+ = \mathbb{R}^+ \times \mathbb{R}^+$, we denote $\bar{y} := (y_1, -y_2)$ and $\tilde{y} := (-y_1, y_2)$. Due to odd symmetry, (8.2) becomes (we drop t from the notation in this sub-section)

$$u_1(x) = -\int_{D^+} K_1(x,y)\omega(y)dy, \tag{8.10}$$

where

$$K_1(x,y) = \underbrace{\frac{y_2 - x_2}{|x-y|^{2+2\alpha}}}_{K_{11}(x,y)} - \underbrace{\frac{y_2 - x_2}{|x-\tilde{y}|^{2+2\alpha}}}_{K_{12}(x,y)} - \underbrace{\frac{y_2 + x_2}{|x+y|^{2+2\alpha}}}_{K_{13}(x,y)} + \underbrace{\frac{y_2 + x_2}{|x-\bar{y}|^{2+2\alpha}}}_{K_{14}(x,y)}, \tag{8.11}$$

Analyzing (8.11), it is not hard to see that we can split the region of integration in the Biot-Savart law according to whether it helps or opposes the bounds we seek. Define

$$u_1^{bad}(x) := -\int_{\mathbb{R}^+\times(0,x_2)} K_1(x,y)\omega(y)dy \text{ and } u_1^{good}(x) := -\int_{\mathbb{R}^+\times(x_2,\infty)} K_1(x,y)\omega(y)dy.$$

The following two lemmas contain the key estimates.

Lemma 8.4 (Bad part)**.** *Let $\alpha \in (0, \frac{1}{2})$ and assume that ω is odd in x_1 and $0 \le \omega \le 1$ on D^+. If $x \in \overline{D^+}$ and $x_2 \le x_1$, then*

$$u_1^{bad}(x) \le \frac{1}{\alpha}\left(\frac{1}{1-2\alpha} - 2^{-\alpha}\right) x_1^{1-2\alpha}. \tag{8.12}$$

The proof of this lemma uses (8.11) and after cancellations leads to the bound

$$u_1^{bad}(x) \le -\int_{(0,2x_1)\times(0,x_2)} \frac{y_2 - x_2}{|x-y|^{2+2\alpha}}dy, \tag{8.13}$$

which gives (8.12)

In the estimate of the good part, we need to use a lower bound on ω that will be provided by the barrier. Define

$$A(x) := \{y \,:\, y_1 \in (x_1, x_1+1) \text{ and } y_2 \in (x_2, x_2 + y_1 - x_1)\}. \tag{8.14}$$

Lemma 8.5 (Good part)**.** *Let $\alpha \in (0, \frac{1}{2})$ and assume that ω is odd in x_1 and for some $x \in \overline{D^+}$ we have $\omega \ge \chi_{A(x)}$ on D^+, with $A(x)$ from (8.14). There exists $\delta_\alpha \in (0,1)$, depending only on α, such that the following holds.*

If $x_1 \le \delta_\alpha$, then

$$u_1^{good}(x) \le -\frac{1}{6\cdot 20^\alpha \alpha} x_1^{1-2\alpha}.$$

Here analysis of (8.11) leads to

$$u_1^{good}(x) \le \underbrace{-\int_{A_1} \frac{y_2 - x_2}{|x-y|^{2+2\alpha}}dy}_{T_1} + \underbrace{\int_{A_2} \frac{y_2 - x_2}{|x-y|^{2+2\alpha}}dy}_{T_2},$$

with the domains

$$A_1 := \{y \,:\, y_2 \in (x_2, x_2+1) \text{ and } y_1 \in (x_1 + y_2 - x_2, 3x_1 + y_2 - x_2)\},$$
$$A_2 := (x_1+1, 3x_1+1) \times (x_2, x_2+1).$$

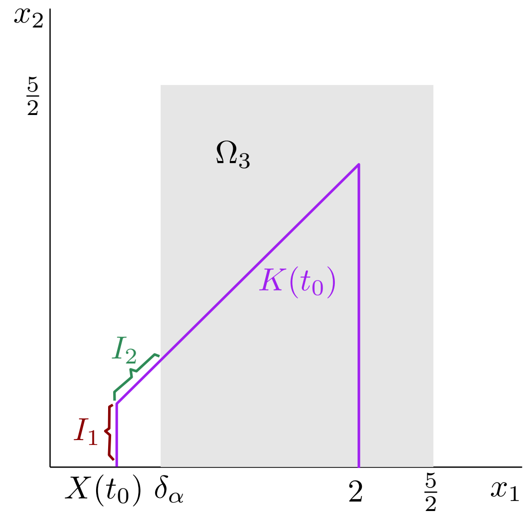

FIGURE 5. The segments I_1 and I_2 and the sets Ω_3 and $K(t_0)$.

The term T_2 can be estimated by Cx_1, since the region of integration A_2 lies at a distance ~ 1 from the singularity. A relatively direct estimate of the term T_1 leads to the result of the Lemma.

A distinctive feature of the problem is that estimates for the "bad" and "good" terms appearing in Lemmas 8.4 and 8.5 above have the same order of magnitude $x_1^{1-2\alpha}$. This is unlike the 2D Euler double exponential growth construction, where we were able to isolate the main term. To understand the balance in the estimates for the "bad" and "good" terms, note that the "bad" term estimate comes from integration of the Biot-Savart kernel over rectangle $(0, 2x_1) \times (0, x_2)$, while the good term estimate from integration of the same kernel over the region A_1 above. When α is close to zero, the kernel is longer range, and the more extended nature of the region A_1 makes the "good" term dominate. In particular, the coefficient $\frac{1}{\alpha}\left(\frac{1}{1-2\alpha} - 2^{-\alpha}\right)$ in front of $x_1^{1-2\alpha}$ in Lemma 8.4 converges to to finite limit as $\alpha \to 0$, while the coefficient $\frac{1}{6 \cdot 20^\alpha \alpha}$ in Lemma 8.5 tends to infinity. On the other hand, when $\alpha \to \frac{1}{2}$, the singularity in the Biot-Savart kernel is strong and getting close to non-integrable. Then it becomes important that the "bad" term integration region contains an angle π range near the singularity, while the "good" region only $\frac{\pi}{4}$. For this reason, controlling the "bad" term for larger values of α is problematic - although there is no reason why there cannot be a different, more clever argument achieving this goal.

It is straightforward to check that the dominance of the "good" term over "bad" one extends to the range $\alpha \in (0, \frac{1}{24})$, and that in this range we get as a result

$$u_1(x,t) \leq -\frac{1}{50\alpha} x_1^{1-2\alpha} \tag{8.15}$$

for $x = (x_1, x_2)$ such that $x_1 \leq \delta_\alpha$ and $x_1 \geq x_2$. A similar bound can be proved showing that

$$u_2(x,t) \geq \frac{1}{50\alpha} x_2^{1-2\alpha} \tag{8.16}$$

for $x = (x_1, x_2)$ such that $x_2 \leq \delta_\alpha$ and $x_1 \leq x_2$.

The proof is completed by a contradiction argument, where we assume that the barrier $K(t)$ catches up with the patch $\Omega(t)$ at some time $t = t_0 < T$ of first contact. Taking ϵ sufficiently small compared to δ_α from Lemma 8.5, we can make sure the contact can only happen on the intervals I_1 and I_2 along the boundary of the barrier $K(t_0)$ appearing on Figure 5. But then bounds (8.15), (8.16) and the evolution of the barrier prescription (8.9) lead to the conclusion that the barrier should have been crossed at $t < t_0$, yielding a contradiction.

9. The SQG equation: smooth solutions

More details on material presented in this section can be found in [29]. As we already mentioned above, until recently, there have been no examples of smooth solutions to the SQG equation exhibiting infinite in time growth of derivatives. The best known result [36] involved only finite time bursts of growth. In this section, we outline the argument of [29] where examples of SQG solutions with infinite - exponential in time - growth of derivatives have been obtained. The construction involves a mix of ideas from [37], from the work of Zlatos [64] yielding exponential in time growth for periodic solutions of the 2D Euler equation, and some new ingredients. The theorem below involves the whole range of the modified SQG equations.

Theorem 9.1. *Consider the modified SQG equations* (8.1) *in periodic setting. For all* $0 < \alpha < 1$, *there exist initial data* ω_0 *such that*

$$\sup_{t \leq T} \|\nabla^2 \omega(\cdot, t)\|_{L^\infty} \geq \exp(\gamma T), \tag{9.1}$$

for all $T > 0$ *and constant* $\gamma > 0$ *that may depend on* ω_0 *and* α. *This constant can be made arbitrarily large by picking* ω_0 *appropriately.*

Note that if $\alpha > 1/2$, the models considered are actually more singular then the SQG equation. Even local well-posedness in this case is not obvious, but has been established in [5]. Also, observe that we do not prove global regularity of the solutions in these examples - solutions that blow up in finite time will also satisfy (9.1).

As before, we will make use of symmetries and assume that the initial data (and so the solution) is odd with respect to both x_1 and x_2. We will also need a certain degenerate structure, with solution vanishing to higher order near the x_2 axis. The following lemma shows that this property is preserved in time.

Lemma 9.2. *Suppose that in addition to being odd in* x_1 *and* x_2 *and periodic, the initial data* ω_0 *also satisfies* $\partial_{x_1}\omega_0(0, x_2) = 0$ *for all* x_2. *Then the solution* $\omega(x, t)$, *while it remains smooth, also satisfies* $\partial_{x_1}\omega(0, x_2, t) = 0$.

The lemma is proved by differentiation of the equation and direct analysis. Note that all even derivatives of ω also vanish when $x_1 = 0$ due to odd symmetry.

Next, we need to carefully analyze the Biot-Savart law, which we state below under assumption of oddness in both x_1 and x_2.

$$u_1(x) = \int_0^\infty \int_0^\infty \left(\frac{x_2 - y_2}{|x-y|^{2+2\alpha}} - \frac{x_2 - y_2}{|\tilde{x}-y|^{2+2\alpha}} - \frac{x_2 + y_2}{|\bar{x}-y|^{2+2\alpha}} + \frac{x_2 + y_2}{|x+y|^{2+2\alpha}} \right) \omega(y)\, dy_1 dy_2, \tag{9.2}$$

$$u_2(x) = -\int_0^\infty \int_0^\infty \left(\frac{x_1 - y_1}{|x-y|^{2+2\alpha}} - \frac{x_1 - y_1}{|\bar{x}-y|^{2+2\alpha}} - \frac{x_1 + y_1}{|\tilde{x}-y|^{2+2\alpha}} + \frac{x_1 + y_1}{|x+y|^{2+2\alpha}} \right) \omega(y)\, dy_1 dy_2. \tag{9.3}$$

Here $\tilde{x} = (-x_1, x_2)$, $\bar{x} = (x_1, -x_2)$, and the function ω is extended to the entire plane by periodicity. We will later see that the integral converges absolutely at infinity if $\alpha > 0$. Near the singularity $x = y$, the convergence is understood in the principal value sense if $\alpha \geq 1/2$. In what follows, we will denote the kernels in the integrals (9.2), (9.3) by $K_1(x, y)$ and $K_2(x, y)$ respectively.

Let $L \geq 1$ be a constant that we will eventually choose to be large enough. The first estimate addresses the contribution of the near field $y_1, y_2 \leq L|x|$ to the Biot-Savart law provided that we have control of $\|\nabla^2\omega\|_{L^\infty}$. All the inequalities we show in the rest of this section, similarly to Lemma 9.2, assume that the solution remains smooth at times where these inequalities apply.

Lemma 9.3. *Assume that ω is odd with respect to both x_1 and x_2, periodic and smooth. Take $L \geq 2$, and suppose $L|x| \leq 1$. Denote*

$$u_j^{near}(x) = \int_{[0,L|x|]^2} K_j(x, y)\omega(y)\, dy.$$

Then we have

$$|u_j^{near}(x)| \leq Cx_j|x|^{2-2\alpha}L^{2-2\alpha}\|\nabla^2\omega\|_{L^\infty}. \tag{9.4}$$

The lemma is proved by about a page of estimates. The control of the second derivative of ω is used, in particular, to estimate the principal value singularity. The key observation is that in the integral

$$\left| P.V. \int_0^{L|x|} dy_1 \int_0^{2x_2} dy_2 \frac{(x_2 - y_2)(|\tilde{x} - y|^{2+2\alpha} - |x - y|^{2+2\alpha})}{\tilde{x} - y|^{2+2\alpha}|x - y|^{2+2\alpha}} \omega(y, t) \right|$$

the kernel is odd with respect to $y_2 = x_2$ line, so $\omega(y, t)$ can be replaced by $\omega(y_1, y_2, t) - \omega(y_1, x_2, t)$. The latter difference can be estimated using second order derivatives by mean value theorem, and the order of the singularity can be reduced to integrable. There are of course more terms to estimate but their control is more straightforward.

The next result records an important property of the Biot-Savart law that makes contribution of the $L|x| \leq |y| \lesssim 1$ region of the central cell to u_1 and u_2 nearly identical when L is large.

Proposition 9.4. *Let L be a parameter and x be such that $L|x| \leq 1$. Assume that ω is odd with respect to both x_1 and x_2, $\omega(x) \geq 0$ in $[0, \pi)^2$, and is positive on a set of measure greater than $(L|x|)^2$. Let us define*

$$u_j^{med}(x) = \int_{[0,\pi)^2 \setminus [0,L|x|]^2} K_j(x, y)\omega(y)\, dy.$$

Then for all sufficiently large $L \geq L_0 \geq 2$ and x such that $L|x| \leq 1$ we have that

$$1 - BL^{-1} \leq -\frac{u_1^{med}(x)x_2}{x_1 u_2^{med}(x)} \leq 1 + BL^{-1}, \tag{9.5}$$

with some universal constant B.

The bound (9.5) follows from more informative pointwise bound for the Biot-Savart kernel. A direct computation shows that in the region $y_1, y_2 \geq L|x|$, we have

$$K_1(x, y) = -8(1 + \alpha)x_1 y_1 y_2 |y|^{-4-2\alpha}(1 + f_1(x, y)), \tag{9.6}$$

and

$$K_2(x,y) = 8(1+\alpha)x_2y_1y_2|y|^{-4-2\alpha}(1+f_2(x,y)), \tag{9.7}$$

where $|f_{1,2}(x,y)| \le AL^{-1}$ with some universal constant A.

Lemma 9.3 and Proposition 9.4 control contribution to the Biot-Savart law of the central period cell. It turns out that the contribution of the rest of the cells is regular near the origin.

Lemma 9.5. *Suppose that* $|x| \le 1$. *Define*

$$u_j^{far}(x) = \int_{[0,\infty)^2\setminus[0,\pi)^2} K_j(x,y)\omega(y)\,dy.$$

Then

$$|u_j^{far}(x)| \le C(\alpha)x_j\|\omega\|_{L^\infty}. \tag{9.8}$$

The final estimate we need is a lower bound on the absolute value of the velocity components $(-1)^j u_j^{med}$, $j=1,2$, near the origin provided certain assumptions on the structure of vorticity.

Lemma 9.6. *There exists a constant* $1 > \delta_0 > 0$ *such that if* $\delta \le \delta_0$, *the following is true. Suppose, in addition to symmetry assumptions made above, that we have* $1 \ge \omega_0(x) \ge 0$ *on* $[0,\pi)^2$ *and that* $\omega_0(x) = 1$ *if* $\delta \le x_{1,2} \le \pi-\delta$. *Then for all* x *and* $L \ge L_0$ *such that* $L|x| \le \delta$, *we have that*

$$(-1)^j u_j^{med}(x,t) \ge cx_j\delta^{-\alpha}. \tag{9.9}$$

The proof of the lemma uses the area preserving property of the flow and the fact that vorticity is conserved along the trajectories, as well as the estimates (9.6), (9.7).

Now we have all the tools to sketch the proof of Theorem 9.1.

The initial data ω_0 will be chosen as follows. First, as we already discussed, ω_0 is odd with respect to both x_1 and x_2, $1 \ge \omega_0(x) \ge 0$ in $[0,\pi)^2$ and it equals 1 in this region, apart from a region of width $\le \delta$ along the boundary. The parameter $\delta \le \delta_0 < 1$ will be fixed later. We also require $\partial_{x_1}\omega_0(0,x_2) = 0$ for all x_2, a condition that is preserved for all times while the solution stays smooth by Lemma 9.2. Finally, we assume that in a small neighborhood of the origin of order $\sim\delta$ we have $\omega_0(x_1,x_2) = \delta^{-4}x_1^3x_2$. Note that $\partial^2_{x_1}\omega_0(0,x_2) = 0$ by oddness, so this is the "maximal" behavior of ω_0 under our degeneracy condition.

Fix arbitrary $T \ge 1$; for small T the result follows automatically as $\|\nabla^2\omega(\cdot,t)\|_{L^\infty} \ge c\delta^{-2}$ for all times. Take $x_1^0 = e^{-T\delta^{-\alpha/2}}$ and $x_2^0 = (x_1^0)^\beta$ where $\beta > 1$ will be chosen later. Observe that

$$\omega_0(x_1^0,x_2^0) = \delta^{-4}(x_1^0)^{3+\beta} = \delta^{-4}e^{-(3+\beta)T\delta^{-\alpha/2}}.$$

Consider the trajectory $(x_1(t),x_2(t))$ originating at (x_1^0,x_2^0). We will track this trajectory until either time reaches T, or $x_2(t)$ reaches x_1^0, or $\|\nabla^2\omega(\cdot,t)\|_{L^\infty}$ becomes large enough to satisfy the lower bound we seek.

Let us denote

$$T_0 = \min\left(T,\, \min\{t:\, x_2(t) = x_1^0\},\, \min\{t:\, \|\nabla^2\omega(\cdot,t)\|_{L^\infty} \ge \exp(cT)\}\right).$$

Note that for all $t \le T_0$, we have $x_2(t) \le x_1^0$.

The first step is to notice that for all $t \le T_0$, if the contribution of u^{far} and u^{near} ever becomes of comparable size relatively to u^{med}, and if the parameters δ and L are appropriately chosen, then the growth condition we seek must be satisfied. A specific condition sufficient for growth estimate is

$$|u_j^{near}(x(t),t)| + |u_j^{far}(x(t),t)| \geq L^{-1}(-1)^j u_j^{med}(x(t),t). \tag{9.10}$$

This can be derived from Lemma 9.3, Lemma 9.5, Lemma 9.6, and the definition of x_1^0. Hence we can from now on assume that (9.10) never holds for $t \leq T_0$; otherwise we are done.

The second step is to observe that if u^{med} does dominate for $t \leq T_0$ and $T_0 = T$, then the exponential growth that we seek would follow simply from Lemma 9.6 as well as conservation of vorticity along trajectories.

This leaves the most interesting case where $T_0 < T$ due to $x_2(t)$ reaching the value x_1^0. The main danger is that u_2 somehow happens to be much more efficient in pushing the trajectory away from the origin than u_1 in compressing it towards the origin. But such scenario is prevented by Proposition 9.4, which basically says that when $u_{1,2}^{med}$ provide dominant contributions to $u_{1,2}$ then these contributions coincide to the main order, and the trajectory is almost precisely a hyperbola. Here is a sketch of the detailed estimate. Using that $u_{1,2}^{med}$ give dominant contributions to $u_{1,2}$ and Proposition 9.4 one can obtain

$$-\frac{u_1(x(t),t)}{x_1(t)} \geq (1-2BL^{-1})\frac{u_2(x(t),t)}{x_2(t)} \tag{9.11}$$

provided that $B > 2$ and L is sufficiently large that can always be arranged. Therefore

$$\frac{x_1^0}{x_1(T_0)} = e^{-\int_0^{T_0} \frac{u_1(x(t),t)}{x_1(t)}\,dt} \geq e^{(1-2BL^{-1})\int_0^{T_0} \frac{u_2(x(t),t)}{x_2(t)}\,dt} =$$

$$\left(\frac{x_2(T_0)}{x_2^0}\right)^{1-2BL^{-1}} = (x_1^0)^{(1-\beta)(1-2BL^{-1})}.$$

Here we used that $x_2^0 = (x_1^0)^\beta$ and $x_2(T_0) = x_1^0$. It follows that

$$x_1(T_0) \leq (x_1^0)^{\beta(1-2BL^{-1})+2BL^{-1}}.$$

This implies that

$$\|\partial^2_{x_1x_1}\omega(\cdot,T_0)\|_{L^\infty} \geq 2\omega(x_1(T_0),x_2(T_0),T_0)x_1(T_0)^{-2} \geq \delta^{-4}(x_1^0)^{3+\beta-2\beta(1-2BL^{-1})} \geq$$

$$\delta^{-4}(x_1^0)^{3-\beta+4\beta BL^{-1}} = \delta^{-4}e^{\delta^{-\alpha/2}(\beta-3-4\beta BL^{-1})T}.$$

Now one select β (say $\beta = 5$ would work), L, and δ so that all parts of the argument are valid, obtaining exponential growth we seek in this final step as well.

Acknowledgement. The author acknowledges partial support of the NSF-DMS grant 1848790, and thanks the organizers of the 2019 CIME summer school on fluid mechanics for the kind invitation to give lectures and excellent organization.

References

[1] H. Bahouri, J.-Y. Chemin, *Équations de transport relatives á des champs de vecteurs nonLipschitziens et mécanique des uides. (French) [Transport equations for non-Lipschitz vector Fields and fluid mechanics],* Arch. Rational Mech. Anal., **127** (1994), no. 2, 159–181

[2] J.T. Beale, T. Kato and A. Majda, *Remarks on the breakdown of smooth solutions of the 3D Euler equations,* Commun. Math. Phys. **94** (1984), 61–66

[3] A. Bertozzi and P. Constantin, *Global regularity for vortex patches,* Comm. Math. Phys., **152** (1993), 19–28

[4] M. P. Brenner, S. Hormoz and A. Pumir, *Potential singularity mechanism for the Euler equations,* Phys. Rev. Fluids **1** (2016), 084503

[5] D. Chae, P. Constantin, D. Cordoba, F. Gancedo and J. Wu, *Generalized surface quasi-geostrophic equations with singular velocities,* Comm. Pure Appl. Math. **65** (2012), no. 8, 1037–1066

[6] J.-Y. Chemin, *Persistance de structures geometriques dans les fluides incompressibles bidimensionnels,* Annales de l'École Normale Supérieure, **26** (1993), 1–26

[7] J. Chen and T. Hou, *Finite time blowup of 2D Boussinesq and 3D Euler equations with $C^{1,\alpha}$ velocity and boundary,* preprint arXiv:1910.00173

[8] J. Chen, T. Hou, and D. Huang, *On the finite time blowup of the De Gregorio model for the 3D Euler equation,* preprint arXiv:1905.06387

[9] K. Choi, A. Kiselev and Y. Yao, *Finite time blow up for a 1D model of 2D Boussinesq system,* Comm. Math. Phys. **334** (2015), no. 3, 1667–1679

[10] K. Choi, T. Hou, A. Kiselev, G. Luo, V. Sverak and Y. Yao, *On the finite-time blowup of a 1D model for the 3D axi-symmetric Euler equations,* Commun. Pure Appl. Math., **70** (2017), 2218–2243

[11] E. A. Coddington and N. Levinson, *Theory of Ordinary Differential Equations,* New York: McGraw-Hill, 1955

[12] P. Constantin, A. Majda and E. Tabak. *Formation of strong fronts in the 2D quasi-geostrophic thermal active scalar*. Nonlinearity **7**, (1994), 1495–1533

[13] D. Cordoba, *Nonexistence of simple hyperbolic blow up for the quasi-geostrophic equation*, Ann. of Math., **148**, (1998), 1135–1152

[14] D. Cordoba and C. Fefferman, *Growth of solutions for QG and 2D Euler equations,* J. Amer. Math. Soc. **15** (2002), 665–670

[15] D. Cordoba, M.A. Fontelos, A.M. Mancho, and J.L. Rodrigo, *Evidence of singularities for a family of contour dynamics equations,* Proc. Natl. Acad. Sci. USA **102** (2005), 5949-–5952

[16] S. Denisov, Infinite superlinear growth of the gradient for the two-dimensional Euler equation, Discrete Contin. Dyn. Syst. A, 23 (2009), no. 3, 755–764

[17] S. Denisov, *Double-exponential growth of the vorticity gradient for the two-dimensional Euler equation,* Proc. Amer. Math. Soc. **143** (2015), no. 3, 1199–1210

[18] T. Do, A. Kiselev, and X. Xu, *Stability of blow up for a 1D model of axi-symmetric 3D Euler equation,* Journal of Nonlinear Science **28** (2018), 2127–2152

[19] A. Einstein, "The causes of the formation of meanders in the courses of rivers and of the so-called Baer's law", Die Naturwissenschaften 14 (1926); English translation in *Ideas and Opinions*, 1954; availble online at `http://people.ucalgary.ca/kmuldrew/river.html`

[20] W. E, K. Khanin, A. Mazel, and Ya. Sinai, *Invariant measures for Burgers equation with stochastic forcing,* Annals of Math. **151** (2000), no. 3, 877–960

[21] T. Elgindi and I.-J. Jeong, *Finite-tim singularity formation for strong solutions to the Boussinesq system,* preprint arXiv:1708.02724

[22] T. Elgindi and I.-J. Jeong, *Finite-time Singularity formation for Strong Solutions to the axi-symmetric 3D Euler Equations,* preprint arXiv:1802.09936

[23] T. Elgindi, *Finite-time singularity formation for $C^{1,\alpha}$ solutions to the incompressible Euler equations on* $\mathbb{R}^3$, preprint arXiv:1904.04795

[24] A. Enciso, M.A. García-Ferrero, D. Peralta-Salas, *The Biot-Savart operator of a bounded domain,* J. Math. Pures Appl. **119** (2018) 85–113

[25] L. Euler, *Principes généraux du mouvement des fluides,* Mémoires de L'Académie Royale des Sciences et des Belles-Lettres de Berlin **11** (4 September 1755, printed 1757), 217–273

[26] U. Frisch, *Turbulence. The legacy of A. N. Kolmogorov,* Cambridge University Press, Cambridge, 1995

[27] F. Gancedo, *Existence for the α-patch model and the QG sharp front in Sobolev spaces,* Adv. Math., **217** (2008), 2569–2598

[28] F. Gancedo and N. Patel, *On the local existence and blow-up for generalized SQG patches,* preprint arXiv:1811.00530

[29] S. He and A. Kiselev, *Small scale creation for solutions of the SQG equation,* preprint arXiv:1903.07485
[30] I. Held, R. Pierrehumbert, S. Garner and K. Swanson. *Surface quasi-geostrophic dynamics*, J. Fluid Mech., 282, (1995), 1–20
[31] V. Hoang, B. Orcan, M. Radosz and H. Yang, *Blowup with vorticity control for a 2D model of Boussinesq equations,* Journal of Differential Equations **264** (2018), 7328–7356
[32] E. Hölder, *Über die unbeschränkte Fortsetzbarkeit einer stetigen ebenen Bewegung in einer unbegrenzten inkompressiblen Flüssigkeit,* Math. Z. **37** (1933), 727–738
[33] T. Y. Hou and P. Liu, *Self-similar singularity of a 1D model for the 3D axisymmetric Euler equations,* Res. Math. Sci. **2** (2015), Art. 5, 26 pp.
[34] A. Kiselev, *Small scales and singularity formation in fluid dynamics,* preprint arXiv:1807.00184, to appear at Proceedings of the ICM 2018, Rio de Janeiro
[35] A. Kiselev and C. Li, *Global regularity and fast small scale formation for Euler patch equation in a smooth domain,* preprint arXiv:1806.07744, to appear at Commun. PDE
[36] A. Kiselev and F. Nazarov, *A simple energy pump for the periodic 2D surface quasi-geostrophic equation,* 175–179, Abel Symp., 7, Springer, Heidelberg, 2012
[37] A. Kiselev and V. Sverak, *Small scale creation for solutions of the incompressible two dimensional Euler equation,* Annals of Math. **180** (2014), 1205-–1220
[38] A. Kiselev, L. Ryzhik, Y. Yao and A. Zlatos, *Finite time singularity for the modified SQG patch equation,* Ann. of Math. **184** (2016), no. 3, 909–948
[39] A. Kiselev, J.-M. Roquejoffre and L. Ryzhik, *Appetizers in Nonlinear PDE,* draft available at http://math.stanford.edu/~ryzhik/STANFORD/STANF272-15/notes-272-15.pdf
[40] A. Kiselev, Y. Yao and A. Zlatos, *Local regularity for the modified SQG patch equation,* Commun. Pure Appl. Math. **70** (2017), 1253–1315
[41] A. Kiselev and C. Tan, *Finite time blow up in the hyperbolic Boussinesq system,* Adv. Math. **325** (2018), 34—55
[42] A. Kiselev and H. Yang, *Analysis of a singular Boussinesq model,* Research in Mathematical Sciences **6** (2019), no. 1, Paper No. 13, 16 pp
[43] G. Luo and T. Hou, *Toward the finite-time blowup of the 3d axisymmetric Euler equations: A numerical investigation,* Multiscale Model. Simul., **12**(4) (2014), 1722–1776
[44] A. Majda and A. Bertozzi, *Vorticity and Incompressible Flow,* Cambridge University Press, 2002
[45] A. Majda, *Introduction to PDEs and Waves for the Atmoshpere and Ocean,* Courant Lecture Notes in Mathematics, AMS 2003
[46] C. Marchioro and M. Pulvirenti, *Mathematical Theory of Incompressible Nonviscous Fluids,* Applied Mathematical Sciences, **96**, Springer-Verlag, New York, 1994
[47] Y. Motoori and S. Goto, *Generation mechanism of a hierarchy of vortices in a turbulent boundary layer,* J. Fluid Mech. **865** (2019), 1085–1109
[48] C. Muscalu and W. Schlag, *Classical and Multilinear Harmonic Analysis,* Cambridge University Press, 2013
[49] N. S. Nadirashvili, *Wandering solutions of the two-dimensional Euler equation, (Russian)* Funktsional. Anal. i Prilozhen., 25 (1991), 70–71; translation in Funct. Anal. Appl., 25 (1991), 220–221 (1992)
[50] J. Pedlosky, *Geophysical Fluid Dynamics,* Springer, New York, 1987
[51] L. Prandtl, *Essentials of Fluid Dynamics,* London (Blackie and Son), 1952
[52] J.L. Rodrigo, *On the evolution of sharp fronts for the quasi-geostrophic equation,* Comm. Pure Appl. Math., **58**, (2005), 821–866
[53] E.-W. Saw et al, *Experimental characterization of extreme events of inertial dissipation in a turbulent swirling flow,* Nature Communications **7** (2016), Article number: 12466
[54] R. K. Scott and D. G. Dritschel, *Numerical Simulation of a Self-Similar Cascade of Filament Instabilities in the Surface Quasigeostrophic System,* Phys. Rev. Lett. **112** (2014), 144505
[55] R. K. Scott and D. G. Dritschel, *Scale-invariant singularity of the surface quasigeostrophic patch,* J. Fluid Mech. **863** (2019), R2, 12 pp. 86-08
[56] T. Tao, *Finite time blowup for an averaged three-dimensional Navier-Stokes equation,* J. Amer. Math. Soc., **29** (2016), 601–674

[57] T. Tao, *Finite time blowup for Lagrangian modifications of the three-dimensional Euler equation,* Ann. PDE **2** (2016), no. 2, Art. 9, 79 pp

[58] C. Villani, *The age of the Earth: When the Earth was too young for Darwin,* ICM 2018 lecture, https://www.youtube.com/watch?v=ObSv67R-uyg

[59] W. Wolibner, *Un theorème sur l'existence du mouvement plan d'un uide parfait, homogène, incompressible, pendant un temps infiniment long (French),* Mat. Z., **37** (1933), 698–726

[60] X. Xu, *Fast growth of the vorticity gradient in symmetric smooth domains for 2D incompressible ideal flow,* Journal of Mathematical Analysis and Applications **439.2** (2016), 594–607

[61] V.I. Yudovich, *The loss of smoothness of the solutions of the Euler equation with time (Russian),* Dinamika Sploshn. Sredy **16** Nestacionarnye Probelmy Gidordinamiki (1974), 71–78

[62] V. I. Yudovich, *On the loss of smoothness of the solutions of the Euler equations and the inherent instability of flows of an ideal fluid,* Chaos, **10** (2000), 705–719

[63] V.I. Yudovich, *Eleven great problems of mathematical hydrodynamics,* Moscow Mathematical Journal, **3**(2003), 711–737

[64] A. Zlatos, *Exponential growth of the vorticity gradient for the Euler equation on the torus,* Adv. Math. **268** (2015), 396–403